ADVANCED INTELLIGENT SYSTEMS
Open Access
www.advintellsyst.com

Advances in 3D and 4D Printing of Soft Robotics and Their Applications

*Hao Liu, Changchun Wu, Senyuan Lin, James Lam, Ning Xi, and Yonghua Chen**

Soft robots inspired by natural organisms exhibit unprecedented deformation abilities for diverse applications leveraging various smart materials, intelligent structures, and actuation principles. At the same time, advancements in 3D printing technology empower contemporary 3D printers with higher resolution, faster printing speed, and a broader selection of materials. The progression of 3D printing technologies offers additional avenues for fabricating soft robots, facilitating their practical utilization, and commercialization. This review summarizes fundamental 3D printing principles, encompassing fused filament fabrication, direct ink writing, vat photopolymerization, material jetting, and selective laser sintering and emphasizing their capabilities in material selection, multimaterial printability, soft robot fabrication, and smart material printing. This article is concluded with applications of 3D- and 4D-printed soft robots and perspective on future designs and fabrication strategies is offered. This article bridges the gaps between soft polymers, 3D printing technologies, soft actuators, and robotic applications, providing guidance for multidisciplinary researchers in the domains of 3D printing and soft robotics.

1. Introduction

Soft robots demonstrate exceptional adaptabilities that are difficult for traditional rigid robots composed of rigid linkages and rotational joints. Benefiting from their inherent flexibility and compliance, soft actuators can interact safely with delicate objects or collaborate effectively with humans. Furthermore, the multiple degrees of freedom (DOF) and large shape-morphing abilities enable soft robots to adapt to unstructured and dynamic environments. The emergence of soft robots also breaks the cognitive limitations of engineers in design, moving beyond conventional mechanical transmission to explore a diverse range of fascinating flexible structures, smart materials, and intelligent actuation principles. While significant advancements have been made in soft robot design in recent years, challenges persist in industrial applications and daily human activities due to requirements of complex perception, robust control, high comprehensive performance, and complicated manufacturing processes.[1–4]

Inspired by biological features, researchers have proposed various soft actuators, including soft pneumatic actuators (SPAs), electroactive polymers (EAPs), and stimulus-responsive materials. These actuators can produce reversible deformations such as expanding, extending, bending, contracting, twisting, or hybrid deformations to satisfy requirements in diverse application scenarios.[5–8] Soft actuators made of smart materials can be activated by various stimuli, like temperature, magnetic fields, light, acoustic signals, humidity, and chemicals, catering to specific application needs such as drug delivery.

Soft robots can be constructed from a variety of soft materials, including rubber elastomers, hydrogels, fabrics, plastic films, and other synthetic materials.[9] The rapid advancements in additive manufacturing (AM) technology, particularly in printing resolution, material diversity, and forming speed, have led to significant progress in the fabrication processes of various soft actuators and soft robotic systems. Intelligent manufacturing techniques such as 3D printing have paved the road for the wide applications of soft robots.

We retrieved and analyzed a total of 3556 articles published between 2011 and 2024 from the Web of Science (WoS) using the keywords "3D printing" (or "4D printing" or "additive manufacturing") and "soft robotics" (or "soft devices"), as depicted in **Figure 1**.[10] The results were filtered to include proceedings, articles, and review articles. This search query was conducted on December 28, 2024. The chronological bibliometric analysis indicates a notable surge in publications concerning 3D-printed soft robots since 2018 (Figure 1A). Moreover, citations related to this topic have increased faster than the publications, signifying high attention to 3D-printed soft robots in multidisciplinary fields (Figure 1B). Figure 1C,D showcase the universities and countries with the highest publication volumes. The United States of America (USA) and the People's Republic of China lead in publications on 3D printing soft robots, holding the first and second positions, respectively.

H. Liu, C. Wu, S. Lin, J. Lam, Y. Chen
Department of Mechanical Engineering
The University of Hong Kong
Hong Kong 999077, China
E-mail: yhchen@hku.hk

N. Xi
Department of Data and Systems Engineering
The University of Hong Kong
Hong Kong 999077, China

The ORCID identification number(s) for the author(s) of this article can be found under https://doi.org/10.1002/aisy.202400699.

DOI: 10.1002/aisy.202400699

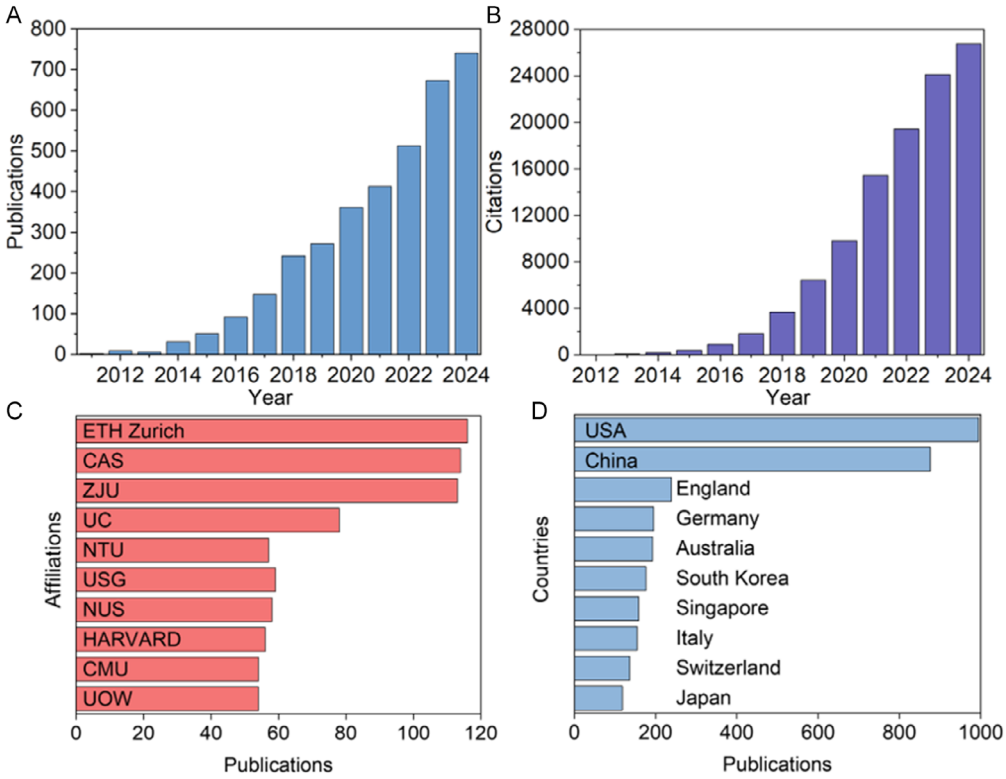

Figure 1. Bibliometric analysis of 3D-printed soft robots. A) Number of publications in recent years. B) Number of citations for the past 14 years. C) Top ten research institutions ranked by the number of publications. The full names of the institutions are illustrated in the nomenclature section. D) Top ten countries according to the number of publications.

This review article systematically examines state-of-the-art 3D printing technologies, focusing on printable materials and the capabilities of multimaterial printing. Furthermore, it summarizes 3D-printed soft robots and 4D-printed actuators based on the various 3D printing methodologies and working principles. The article emphasizes the applications of 3D-printed soft robots in the fields of soft grippers, artificial muscles, locomotion robots, biomedical devices, and sensor-integrated actuators. Discussion on the challenges and opportunities associated with 3D-printed soft actuators and their applications is provided. Finally, the article outlines the prospects of 3D-printed soft robots in practical utilization.

2. Soft Matter and Additive Manufacturing Technologies

According to the elastic range of organs and tissues in natural creatures, scientists define materials with Young's modulus in the range of 10^4–10^9 Pa as soft materials.[11] In contrast to rigid plastics and metals, soft materials possess outstanding deformability. Due to the viscoelastic deformation under forces, soft matters are traditionally fabricated by coating, injection molding, extrusion, and soft lithography.[12–14] These conventional machining methods often struggle to address the complexities of multimaterial systems and complex structural designs. The advent of 3D printing, or AM, has revolutionized the concept of mechanical engineers in designing structures, simplified the product design process, reduced the prototype iteration times, and broken down the limitations of structure design and material combinations.

3D printing technology simplifies the manufacturing process by directly translating computer-aided design (CAD) models into 3D physical objects without the specialized technical training required by traditional machine tools. Different from traditional machining methods such as turning, milling, drilling, planing, boring, and electrical discharge machining, which carve parts from specific blanks to achieve the desired shape, 3D printing technology operates by slicing the CAD model and constructing it layer by layer through the print head or laser head to fabricate 3D objects. 3D printing technology can be divided into seven categories based on the forming principle: material extrusion (MEX), vat photopolymerization (VPP), material jetting (MJ), powder bed fusion (PBF), binder jetting, energy deposition, and sheet lamination.[15] Sheet lamination processes typically use ultrasonic welding to bond metal sheets together or glue cardboard to form a 3D structure. Laminated objects are usually used for artworks and visual structures that are not suitable for structural purposes. Although researchers tried to bond the thermoplastic polyurethane (TPU)-coated baric layer together by hot pressing to design fabric-based soft actuators and they bonded fabric with 3D-printed TPU parts by hot pressing to achieve large-scale soft robot designs,[16–18] the above two-sheet lamination processes have a low degree of automation and involve

significant manual operations. Directed energy deposition employs an energy source like plasma arcs, lasers, or electron beams to melt materials while depositing them through a nozzle, commonly used in metal and alloy fabrication. Additionally, binder jetting uses liquid bonding agents to selectively bind powdered materials, frequently employed in metal, ceramic, and sand molds. Considering that soft robots primarily consist of soft polymers, this article focuses on the remaining four printing technologies. This section delves into their capability for material diversity and multimaterial printing, serving as a guide for engineers in selecting the appropriate AM approach for soft device production.

The printability of various materials using different 3D printing mechanisms, encompassing soft materials, smart materials, composites, and multimaterials, is summarized in **Figure 2**. The ease of printing these materials through 3D printing principles is categorized into four levels, ranging from easy to difficult. Level 1: Materials that can be easily printed using 3D printing technology. Abundant literature supports the maturity and reliability of this approach. Level 2: Materials that can be processed using 3D printing technology, but there is limited research on the use of this printing method. Researchers may need to prepare and adjust precursor materials independently. For instance, incorporating nanoparticles into the resin may impact flow properties, light absorption, and may lead to particle agglomeration, affecting print quality. Notably, using VPP to print composites for soft robots has gained significant attention in recent years.[19] Level 3: Printing this material using this 3DP method is challenging, necessitating customized 3D printers or printed objects showing poor mechanical properties. Although there are commercial silicone elastomer inks for MJ, and properties (e.g., ductility and service life) of the MJ-printed parts are far weaker than other fabrication methods, multimaterial printing is difficult for VPP and selective laser sintering (SLS), as their common printing processes are conducted in a single vat. Level 4: Currently, no literature or theory proves that this 3DP method can print this material. For example, fused filament fabrication (FFF) and SLS cannot print thermoset polymers like silicone rubbers, liquid crystal elastomers (LCEs), and hydrogels. The details and existing challenges of 3D printing these materials are expounded upon in subsequent sections.

2.1. Fused Filament Fabrication (FFF)

MEX is a common AM mechanism. Materials are extruded from nozzles to generate a continuous semiliquid filament by applying pressure on it using gears, syringes, and screws, selectively depositing material on a platform to generate one layer of the target 3D object. Throughout production, the extruder moves relative to the print platform in the x–y–z directions, depositing the filament to the platform. After completing one layer of material build-up, the extruder rises, or the platform descends to start the next layer of printing. This printing process continues until the entire component is completed.

2.1.1. Filaments of FFF

The primary and widely used MEX-based 3D printing method is FFF, also called fused deposition modeling (FDM). In FFF technology, thermoplastic 3D printing filaments are melted by a heating block and stacked layer by layer on a platform through a nozzle to form 3D objects.

FFF-based 3D printers can print a broad spectrum of thermoplastics including rigid polymers like polylactic acid (PLA), polyethylene terephthalate glycol (PETG), polyether ether ketone (PEEK), acrylonitrile-butadiene-styrene (ABS), and Nylon.[20–22] Additionally, they can print elastic polymers

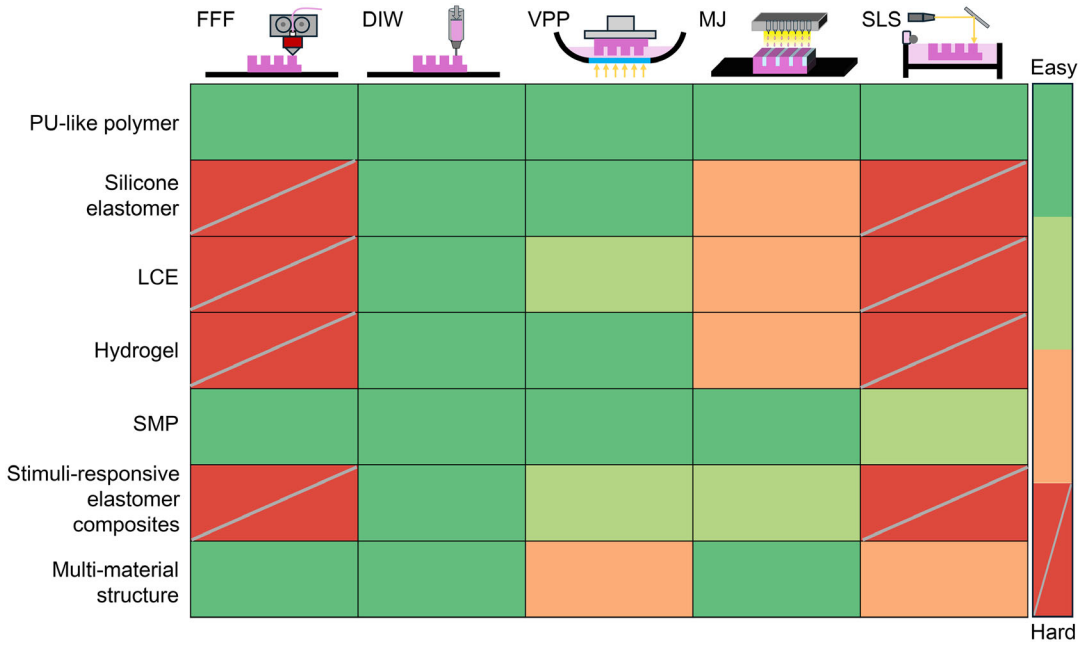

Figure 2. Capabilities of each 3D printing technology for different soft materials.

such as TPU,[23,24] and water-soluble synthetic polymers, like polyvinyl alcohol (PVA), etc.[25] The most common 4D printing material in FFF technology is shape memory polymer (SMP),[26] which can reduce its stiffness when heated and then deform under force and return to its original shape when heated again. This process is called the shape memory effect (SME).

Engineers have explored the intermixing of standard thermoplastic polymers and functional particles or fibers to create composites with special functions. Yang et al. devised a robotic finger joint by printing SMP and conductive TPU (CTPU) in one piece via FFF and embedded the finger joint in the bottom of a fiber-reinforced bending actuator to improve the actuator load-bearing capacity.[27] A commercial CTPU, which is electrically conductive by doping the TPU with carbon black (CB) particles, can produce Joule heat to change the SMP's stiffness and act as a position sensor. In addition, because thermoplastic polymers are inherently softened by heat, researchers embedded conductive PLA (CPLA) into the bottom of the SPA to adjust the stiffness of the actuator in different positions.[28] Chatzipirpiridis et al. investigated the 3D printing of thermoplastic-bonded magnetic composites (TBMC) made of polyamide (PA)-containing magnetic particles. Based on the TBMC,[29] researchers constructed a magnetic planetary gear system featuring a TBMC ring gear, a nonmagnetic PLA sun gear, and five nonmagnetic PLA planet gears. When a magnetic field is applied, the TBMC ring gear rotates to propel the entire planetary gear system at a frequency of 8 Hz.

2.1.2. Multimaterial Printing of FFF

Multimaterial 3D printing has always been a concern for engineers when choosing a processing method. Most of the FFF printers implement multimaterial printing through multiple extruders. A common approach is the dual-extruder 3D printer, capable of printing two materials in a single printer. Recently, Bambu Lab proposed an automatic material system that could print a maximum of 16 colors through a single nozzle (Bambu Lab X1-Carbon Combo, Bambu Lab, China). For FFF 3D printers, printing flexible (TPU) and rigid materials (PETG, PLA, and ABS) together remains a challenge. Geometrical locking is a common strategy used to bond two incompatible materials together. Wrapping-based fabrication strategy is an accessible method to print soft–rigid hybrid structures, leveraging rigid material as backbone and soft material as flexible joints.[30]

Generally, FFF is a user-friendly printing method with low cost, easy operation, and safe materials. The inherent printing mechanism also limits the material selection and mechanical properties of finished products. Only thermoplastic polymers are compatible with the FFF process. The tensile strength of the FFF-fabricated objects in the *z*-axis is significantly lower than in other directions, indicating anisotropy. With the iteration of 3D printing filaments and the optimization of extruders, FFF can print increasingly soft filaments (TPU 55A). An overly soft TPU filament may lead to nozzle blockages or extruder gear slippage during printing. Overall, printing low-hardness, airtight, and robust TPU at high speeds is still an important research gap for soft robot commercialization.

2.2. Direct Ink Writing (DIW)

The direct ink writing (DIW) method, also known as liquid deposition modeling, can print extra soft materials and provides more possibilities for 3D printed soft robots. The layer-by-layer mode of DIW operation is the same as FFF, but with a more diverse range of MEX methods, such as air pressure, pistons, or screws used to extrude the precursor ink. Depending on the properties of the printed material, some curing process (e.g., thermal curing and photopolymerization) is usually required after the deposition of the ink.

2.2.1. Inks of DIW

Different from FFF, which is limited to printing thermoplastic polymers, DIW can print almost any material as long as the precursor ink can be engineered to demonstrate appropriate rheological behavior.[31] High-quality DIW printing requires a continuous and smooth ink extrusion process. The rheological behavior of ink directly affects its printability and shape fidelity, influencing the shape change of the printed object after deposition, drying, and postprocessing.[32] Achieving high-quality, reliable, and consistent printing requires that the ink flow during extrusion rapidly transforms into a solid (or gel) state after deposition onto the platform, that is, exhibiting shear thinning (also called pseudoplastic). Shear thinning is a non-Newtonian fluid characteristic where the viscosity decreases under shear stress. For materials that do not meet the rheological properties of the traditional DIW process, adding functional particles to the ink matrix or using additional equipment to achieve an in situ cure of the ink was done. For instance, mixing CB into silicones can impede curing depth, improve visual monitoring ability, lessen electrostatic repulsion, and enable curing under ultraviolet (UV) light to solve the silicone slumping under its weight.[33]

By controlling ink composition, printing parameters, and curing conditions, DIW technology is widely used to print polymers, ceramics, metals, cement, composites, biological tissues, and even food.[34–40] Polymer-based materials are particularly integral to soft robot manufacturing, including polymer resins, hydrogels, silicones, and their composites. DIW can print thermoplastic polymers (like PLA) at room temperature using the solvent-cast direct-write (SC-DW) fabrication method. The SC-DW consists of the robotically controlled microextrusion of a concentrated polymer solution ink filament, combined with rapid solvent (dichloromethane, DCM) evaporation after the filament exits the micronozzle.[41] Postiglione et al. experimented with mixing multiwalled carbon nanotubes (CNTs), PLA, and DCM to form a novel composite and printed the PLA composite with conductive properties by SC-DW.[42] Notably, DIW allows the thermoplastic polymer to contain higher concentrations of nanofillers for better conductivity, avoiding nozzle plugging compared to FFF.[43] Thermoset materials have attracted the attention of researchers due to their excellent interlayer bonding strength and excellent mechanical properties. Chandrasekaran et al. created a cyanate ester (CE) thermoset polymer ink by adding silica nanoparticles for shear thinning behavior.[44] CE thermoset polymer can withstand elevated temperatures up to 428 °C under thermo-oxidative conditions. DIW demonstrates broad material

selectivity in printing elastomeric polymers. Chen et al. synthesized thixotropic inks by a simple one-pot process dispersing nanoclay and silica nanoparticles in a polyurethane suspension and printed mechanically robust TPU foam.[45] The most exciting aspect of DIW technology is its ability to print highly deformable materials such as silicone elastomers and hydrogels.[46–48]

2.2.2. Multimaterial Printing of DIW

Similar to FFF, DIW enables multimaterial printing with multiple printheads to build complex systems.[49] DIW can print multimaterial structures with one nozzle and multiple ink cartridges.[50–52] Due to the structural similarity between FFF and DIW printers, it is feasible to integrate both solutions into a single equipment.[53] Byrne et al. developed a four-axis 3D printer, combining FFF and DIW capabilities. Unlike conventional FFF printers that deposit fused filament on a platform, the platform of this printer is a rotating cylinder, making it more suitable for printing cylindrical objects. The thermoplastic elastomer fiber is printed using a nozzle that can be heated and the silicone matrix (Dragon skin 10, Smooth-on, USA) is printed using a syringe to mold the fiber-reinforced soft actuator in a single process.[54] In addition, DIW inks are characterized by their fluid state before extrusion, that is, they can be easily mixed to achieve multi-MEX. Ober et al. homogeneously blended two inks with an active mixing printhead and achieved 3D printing of viscoelastic inks with programmable control of local composition.[55] Since the DIW printer can extrude inks through the remote pressure control of the ink extrusion without gear systems, engineers designed a complex coaxial printhead structure to achieve the coextrusion of multiple materials.[56] Mueller et al. fabricated architected lattices composed of multicore–shell struts using tailored coaxial nozzles.[57] Scott et al. reported a multimaterial multinozzle 3D printing (MM3D) approach for voxel programming of material composition, function, and structure.[58] Using MM3D, researchers facilitate seamless, high-frequency switching between up to eight different materials to create voxels with a volume approaching that of the nozzle diameter cubed. Larson et al. presented a rotational multimaterial 3D printing (RM-3DP) platform achieving subvoxel control over the local orientation of azimuthally heterogeneous architected filaments.[59]

DIW can print viscoelastic polymers with an elasticity modulus ranging from 0.02 to 1700 MPa with a resolution of up to 50 μm.[60,61] Although DIW is compatible with a variety of materials, it has a low print speed due to layer-by-layer deposition process and a trade-off between print speed and interface integrity.[62] Another challenge for DIW technology involves the gravitational sagging of long beams when printing overhanging structures, particularly for large elastomeric items.[63] A common approach to print overhangs or cavities is to fill them with sacrificial materials (e.g., water-soluble support) and remove the support in a postprocessing manner to create a specific chamber.[64] In addition, DIW printer can fabricate soft overhanging structures by adjusting the rheology of the ink.[65] Wang et al. demonstrated an omnidirectional printing technique to build a non-coplanar elastic feature without sacrificial materials by adjusting the shear-thinning properties of silicone.[66]

While DIW has demonstrated promise in printing multiple materials, switching between different materials imposes more stringent conditions for rapid changes in printer operating parameters (e.g., pressure, flow rate, printhead travel speed). Furthermore, different drying, curing, and sintering conditions for different materials complicate the manufacturing of some materials in a single-printing process. Notably, benefiting from the multiple materials and dexterous nozzle designs, DIW with subvoxel control shows amazing research potential in soft robot designs.[59]

2.3. Vat Photopolymerization (VPP)

VPP selectively cures liquid photosensitive resins in a vat using specific light (usually UV light) to print the target entities in a layer-by-layer process. Since the introduction of the first stereolithography (SLA) 3D printer in the 1980s, various VPP printing methods were developed by optimizing patterning methods to enhance forming speed and printing resolution. These methods include digital projection lithography (DLP), continuous liquid interface production (CLIP), liquid-crystal display, projection micro-SLA (PμSL), two-photon polymerization (TPP), and volumetric AM (VAM). Except for VAM,[67] most VPP-based printers have similar printable materials, curing setup, and forming processes. These detailed differences and characteristics of VPP printing technologies are systematically summarized in previous articles.[11,68] VPP-based printers adjust the orientation of the light source and support plate based on configuration.

2.3.1. Resins of VPP

VPP typically has two basic requirements for printable materials: photocurability and good fluidity. Based on specific groups and photoinitiators (PIs) reacting under particular lights, photopolymerization mechanisms can be classified as radical polymerization, cationic polymerization, and hybrid (dual-cure) polymerization.[69,70] Photopolymers used for VPP feature a low viscosity enabling homogeneous distribution. The main components of SLA photopolymer resins are monomers/oligomers, PIs, and additives.[71] Monomers (or oligomers) are dominant ingredients of photosensitive resin, influencing the forming speed, geometric accuracy, and mechanical properties of the printed object. The common monomer systems involve radical polymerization of (meth)acrylates,[72] cationic polymerization of epoxides (or vinyl ethers), or a mixture.[73] Compared to MEX, VPP can print fewer types of photopolymers and is weak in printing multimaterials. An increasing number of soft resins have been printed using VPP, including elastomeric resins,[74] silicone elastomers,[75] LCEs,[76] and hydrogels.[77] Using low–molecular-weight oligomers exhibits lower viscosities, but it will lead to low T_g and poor mechanical properties.[78] PIs (like acyl phosphine oxides) create reactive species and react with oligomers and monomers under light irradiation, inducing crosslinking to initiate polymer chain growth. The composition of PIs affects the choice of light source (wavelength and intensity), cure speed, yellowing, and cost.[79] Additives are commonly employed to modify resin properties, including pigmentation, diluents, radical inhibitors, stabilizers, photoabsorbers, and functional

nanoparticles. The diluents can enhance the fluidity of liquid resin, radical inhibitors can control gelation time, stabilizers can prevent overpolymerization by neutralizing reactive species, and photoabsorbers can restrict the curing depth to print thinner layers. Unlike DIW, directly adding functional nanoparticles to the inks, VPP has a weak ability to print composites, mainly caused by the following reasons. 1) Mixing nanoparticles or reinforcement fibers will cause strong light scattering and reduce the transparency of the resin. 2) Adding nanoparticles will increase the viscosity of liquid resin and reduce the printing efficiency. 3) Nanoparticles are prone to settle down during long time use, which will cause an unstable and inhomogeneous structure. But that doesn't mean it's impossible to print composites using VPP.[80]

2.3.2. Multimaterial Printing of VPP

Multimaterial 3D printing using VPP technologies presents major challenges compared to MEX and MJ techniques. Despite this, the exceptional printing resolution of VPP has attracted researchers to explore printing multimaterial structures using VPP technologies. One intuitive approach in VPP multimaterial printing is the rotating disk method (RDM).[81,82] Vats containing different resins are distributed around the platform and rotated to switch between resins or cleaning solutions. To enable multiple-vat VPP printing, modifications are required, such as adding vats on a rotating vat carousel and incorporating washing, curing, and drying devices. However, these modifications also reduced the original forming area.[73] The RDM approach has been refined over time, including redesigning the rotating vat carousel system or integrating an automatic control system, to achieve printing with a wider range of materials, larger forming area, and higher precision.[83,84] A notable limitation of the RDM method is the challenge of cleaning the high-viscosity resin. Frequently switching between resin and cleaning solutions increases printing time, material wastage, and potential crosscontamination.

Another VPP multimaterial printing strategy is known as serve on demand. The multimaterial printing technology based on serve-on-demand strategy provides only the amount of resin needed for each layer. Han et al. used a syringe pump to control monomers in and out of the servo stage and a UV-transparent window through channels on the platform for multimaterial printing.[85] Kowsari et al. demonstrated a DLP-based multimaterial printing system that removes residual liquid resin from the substrate using air jets each time the material is switched without the need for cleaning solutions that would damage the printed features. Material switching is achieved by a translationally movable glass plate attached with optically clear polytetrafluoroethylene (PTFE) silicone-adhesive tape to facilitate the separation of residual liquid resin.[86] In addition, Han et al. presented a novel multimaterial PμSL- (MM-PμSL) system using dynamic fluidic control material switching in vats. Although this method allows for quick switching of resins, contamination between materials is unavoidable.[87] Multimaterial printing is also possible by controlling the wavelength to selectively cure different resins mixed in a single vat.[88]

Overall, VPP has become the most promising 3D printing method in recent years due to its exceptional printing resolution and high mechanical properties in finished products. Although it is not impossible to print multimaterials using VPP technology, it is difficult to realize and inevitably accompanied by a variety of problems such as excessive material consumption, extremely long printing time, and printing defects caused by resin mixing. Therefore, VPP-based multimaterial printing is mostly used in manufacturing small-size items and needs further development to broaden its application scenarios.[89]

2.4. Material Jetting (MJ)

MJ, also named inkjet printing, constructs 3D objects via selectively depositing droplets layer by layer like a traditional 2D printer. MJ printers typically consist of a motion platform, an array of inkjet nozzles, and curing equipment.[90] Depending on the dropping mode of ink, MJ can be categorized into drop-on-demand (DOD) inkjet printing and continuous inkjet (CIJ) printing. The DOD operates at a slower speed but offers higher resolution compared to CIJ. The working principles and more detailed comparisons between the two MJ techniques are discussed in the previous article.[11]

2.4.1. Inks of MJ

In the MJ printing process, two essential materials are required: the building material and the support material. Since the precursor used for MJ printing is a low-viscosity fluid with good flow properties and the resin is deposited on the platform without vat, completely dense gel-like supports are compulsory for overhang regions, which will be removed by chemical solution, heating, or using a high-pressure water jet during postprocessing.[91] MJ has two basic requirements for the two materials: curability and suitable fluid properties to ensure that the liquid flows without splashing when dripping like $1 < Z = \frac{\sqrt{W_e}}{R_e} < 10$ and Weber number $W_e > 4$, where R_e is Reynolds number of inks.[92] However, commercial MJ printers (like PolyJet printers from Stratasys) have closed-loop systems whose availability is limited to proprietary materials. Because the extrusion of liquid inks demands only extremely small nozzles, such as a 0.04 mm nozzle diameter in the Stratasys Objet30 Prime printer, multimaterial prints of inks with varying properties can be easily implemented. Meanwhile, highly concentrated functional fillers (fibers or particles) and large filler particles (>100 nm) tend to cause plugging, limiting the use of MJ when printing composites.

Because of the high resolution and excellent multimaterial printing capabilities, MJ is widely applied in intricate structures. However, commercial MJ inks typically exhibit lower mechanical and thermal performance compared to FFF and VPP. Constrained by surface tension and viscosity, researchers have employed a single-nozzle deposition system to print silicone rubber, limiting printing speed and the capability for multimaterial printing.[93,94] In soft actuator designs, elastomers commonly need to undergo high frequency and large deformation. Printing silicone elastomers with high flexibility and robust mechanical properties and fast fabrication of silicone rubber structures with multimaterials remain significant challenges in MJ.

2.5. Selective Laser Sintering (SLS)

PBF is a 3D printing technique by sintering or melting solid powders using a laser or an electron beam as the energy source. Depending on the material solidification principle, the energy source, and whether a binding agent is used or not, PBF can be categorized into SLS, selective laser melting (SLM), electron beam melting, and multijet fusion. SLS is commonly used in polymer fabrication, so in this article, we use SLS to represent PBF.[95] SLS-based 3D printing technology typically involves three steps: powder deposition, powder solidification, and platform down.

2.5.1. Powders of SLS

Powders for SLS should have good flowability, compactibility, and thermal stability. PBF-based processing platforms are usually placed in a high-temperature sealed chamber to improve printing efficiency, with the chamber temperature slightly lower than the printed material's softening points. Therefore, the powder should have a certain degree of aging stability to ensure that degradation does not significantly occur at high temperatures over a long time, affecting the performance of the finished product. In addition, too small powders can lead to safety hazards, such as dust combustion, explosion, or pneumoconiosis of the operator due to powder escape. The printing resolution of the SLS printer is less than 100 μm owing to the powder size limitation.[96] When printing flexible polymers, the material limitations of the powder are particularly strict. The polymer materials used for SLS are thermoplastic, commonly used TPU (DuraForm Flex).[97] Currently, the softest material that SLS can print is TPU 45A.

2.5.2. Multimaterial Printing of SLS

The powder in SLS is laid down in the bed. The uncured powder can serve as support material after compaction, enabling 100% material utilization but also making multimaterial printing extremely difficult. Whitehead et al. developed a multimaterial printing method using SLS technology via an inverted laser and clear glass plates.[98] They tested a combination of TPU and Nylon due to the similar melting temperature. Powders with different melting temperatures mean high laser system costs, the use of multiple glass plates raises the probability of failures, the inverted platform structure prevents the printer from producing complex 3D structures, and an additional release agent is necessary to avoid connections between the glass plates and the powders.

In general, various solutions have been proposed to solve the SLS multimaterial printing problem in recent years.[95] The printing capacity, efficiency, reliability, and economy of the SLS in multimaterial printing are far worse than other printing methods.

3. 3D-/4D-Printed Soft Actuators

For each 3D printing technique, we classified the printed soft actuators into two groups, namely "3D-printed soft actuators" made of common elastomer polymers and "4D-printed soft actuators" based on smart materials. SPAs and passive deformation structures are common 3D-printed designs using TPU or silicone rubbers. Smart polymers and composites (like SMPs, LCEs, hydrogels, and composites with functional particles) could be printed to complex structures for specific applications, and they can be driven by diverse stimuli as shown in **Figure 3**.

3.1. FFF-Printed Soft Actuators

3.1.1. 3D-Printed Soft Actuators Based on FFF

FFF printers are affordable and meet the needs of most industries and amateurs. However, layer resolution is constrained by the size of the nozzle, usually exceeding 0.078 mm.[99] While employing a smaller nozzle can enhance the surface quality of the printed object, it also increases production time and the risk of nozzle clogging. A common method for improving the quality of thermoplastic filament printing is thermal drying to eliminate moisture from the consumables. Additionally, chemical treatments can improve the surface finish and dimensional accuracy of printed objects. Acetone solvent can improve the tensile strength of ABS materials, and using dichloroethane resulted in a better surface finish.[100]

For SPAs, rough surfaces of 3D printed objects lead to air leakage of the actuator, severely affecting the performance of the actuator, which has plagued engineers over the past decade. A common material used for 3D-printed SPAs is TPU due to its exceptional resilience. One of the simplest ways to enhance the airtightness of 3D-printed SPAs is to increase the wall thickness, fill density, and filament flow of the structural parts or to reduce the layer thickness and printing speed. While this approach can effectively mitigate air leakage, it also constrains the performance of the actuator.[100] Another common way of eliminating surface defects on 3D-printed parts is post-treatment by coating them with a dense elastic film, such as rubbery sealant spray.[101,102] Additionally, a major cause of SPA leakage is weaknesses in the connection of adjacent layers, and a common post-processing method to increase the airtightness of flexible printed materials is heat treatment.[103,104] Kim et al. presented a TPU dual-origami structure with a thin-wall feature that can work under 200 kPa pressure input after heat treatment at 172 °C for 2 h.[105] Using the Eulerian path (a single, continuous toolpath), the SPA with extremely thin walls can be created with a minimum wall thickness of two traces.[106,107] 3D-printed SPAs based on the Eulerian path do not require complex postprocessing to achieve good airtightness, and the thin-wall feature reduces the structural stiffness of the SPA, allowing for flexible designs. Wu developed a vision-based FFF printing for airtight soft actuators without any postprocessing.[108]

The hard materials used in desktop FFF 3D printers (e.g., PLA, PETG) are commonly used to create molds for soft robots due to their cost-effectiveness, ease of handling, minimal postprocessing requirements, and compatibility with silicone rubber. However, molded soft robots require multistep casting, tedious demolding, and sealing, so researchers have invested a lot of effort in one-piece 3D-printed soft robots to automate production. Soft bellow actuator is a hot research topic for FFF-printed SPAs because the deformation of bellow does not require

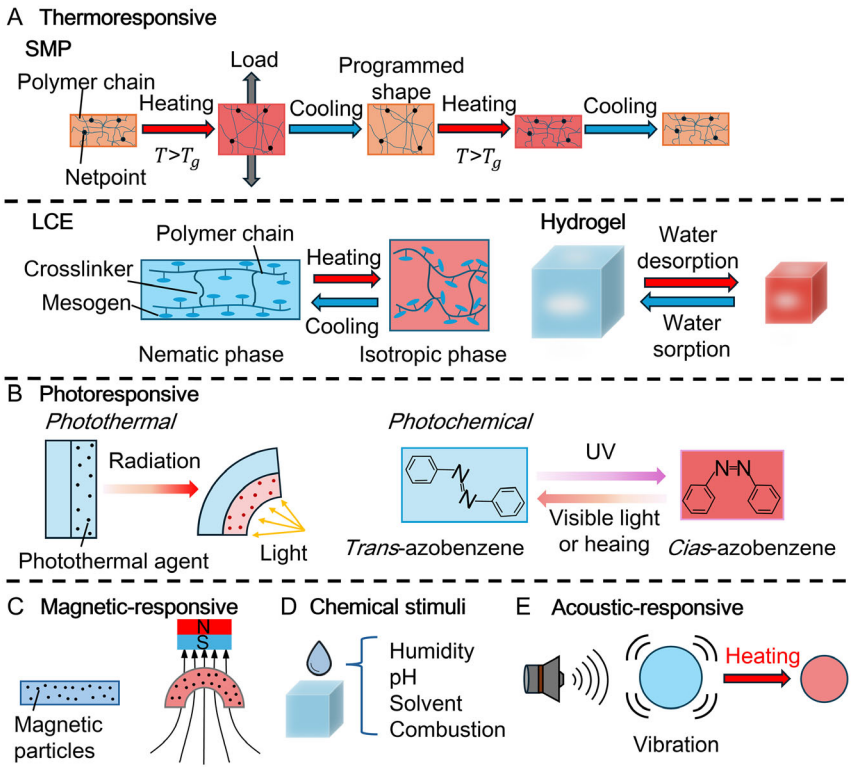

Figure 3. 4D printing smart materials for soft robots. A) Mechanisms of SMP, LCE, and Hydrogel. These actuations can be triggered by temperature change. B) Light-responsive soft actuations. C) Magnetic actuations in soft robots. D) Chemical-responsive actuation. E) Acoustic-responsive soft actuation. The red color implies that the actuators are triggered by environmental stimuli.

large elastic elongation. Tawk et al. designed a 3D-printed bellow actuator named linear soft vacuum actuators (LSOVA) using commercial TPU filament (Ninjiaflex, NinjaTek, USA).[109] By vacuuming the LSOVA, the actuator generates a linear contraction that could be used as an artificial muscle and to drive artificial tendons. Yang et al. presented a fully 3D-printed TPU robotic finger using the classic pneu-net actuator structure.[110] Kresling origami actuator can be created using a similar manufacturing process, which could generate a rotation motion by vacuuming it.[111] 3D-printed Kresling origami actuators were used as soft robotic wrists for robotic manipulation and rotation joints for hexapod robot design.[112]

Apart from the SPAs, some smart structures could adapt to the environment. Inspired by the physiology of fish's tails, scientists proposed the fin ray effect, a triangular structure with hard crossbeams that conform to contacted objects by passive morphing.[113] The most common application of the fin-ray effect is soft robotic grippers, and the whole finger can be made of TPU.[114] Besides, fin ray structures can be utilized to design robotic feet for saving energy and adapting to terrain.[115]

3.1.2. 4D-Printed Soft Actuators Based on FFF

The predominant material used in FFF 4D printing is SMP material (such as PLA). SMP is rigid at room temperature, but when heated above the glass transition temperature (T_g), SMP softens and the bending stiffness of the material decreases by as much as 2–3 orders of magnitude.[116] In this phase, the SMP can be shaped by applying an external force through other actuation methods (like SPA or cable-driven force).[117,118] When the SMP is heated to T_g again following the withdrawal of the external force, the SMP will return to its initial shape due to SME. However, most SMPs only have one-way SME, which limits the application scenarios of SMPs and requires an additional heat source device.[119] One method of integrating heating circuits into SMP structures is to use the coextrusion 4D printing strategy that embeds continuous conductive fibers into thermoplastic SMP.[120] Another way is to use a dual-nozzle FFF 3D printer to print SMP and conductive filament (like graphene PLA) as a whole.[121] Shape-memory polymer composites (SMPCs) were formed by mixing functional nanoparticles, for example, Fe_3O_4 and CNTs into the SMP matrix to obtain excellent electrical conductivity and mechanical properties.[122] Zhao et al. fused Fe_3O_4 nanoparticles and PLA to obtain magnetic stimulated SMPC and designed magnetically driven bioinspired tracheal scaffolds with SME by imitating the porous network structure of glass sponges.[123]

To achieve two-way SME, or reversible SMP, researchers proposed an SMP laminate composite structure.[124] Chen et al. exhibited a laminated SMP composite with two-way SME by bonding a preelongated SMP layer with an unstretched resilient polyurethane film.[125] Cecchini et al. designed a bilayer helical shape soft robot by mimicking Pelargonium appendiculatum Willd seed.[126] The biomimetic seed robot is made of

polycaprolactone (PCL, hygroscopic inactive material) and coaxial electrospinning of hygroscopically active fibers, which can achieve reversible helical morphing triggered by humidity change.

While material selection may constrain design flexibility, FFF is still the most popular 3D printing method due to its affordability and user-friendly operation. Researchers may design soft actuators that morph based on hardness difference if FFF can print superelastic polymer (with a hardness below shore 30A). One potential research direction is using the FFF-based functional composite filaments, such as conductive/magnetic PLA/TPU/SMP, to construct complex robotic systems.

3.2. DIW-Printed Soft Actuators

3.2.1. 3D-Printed Soft Actuators Based on DIW

DIW offers a higher-design DOF of the soft actuator because of its high material diversity. Photocurable silicone inks with adjustable elasticity have been employed to design programmable actuators by mimicking the fibrous architecture of the muscular hydrostats (**Figure 4**A).[127] The bionic fluidic actuators consist of an inflatable soft elastomer chamber and a hard elastomer layer for constraining the chamber deformation. These actuators can achieve bending, torsion, contraction, and localized expansion by adjusting the hard silicone lead angle. Commercial two-part platinum cure silicones (smooth-on, USA) can also be utilized to print pneu-net actuators.[128]

Hydrogel is a promising 3D-printable polymer for soft actuator designs due to its organic-like properties and good biocompatibility. Cheng et al. used an alginate-based naturally occurring ionically percolating network as a versatile rheological modifier to fabricate functional hydrogels. They successfully manufactured an omnidirectional bending hydrogel actuator and a bioengineered robotic heart capable of beating and pumping.[129] Due to the structural simplicity of the DIW printer, exotic components can be obtained by appropriate modifications to the printer structure or by printing on a specific matrix in combination with other fabrication methods. 3D curvature could be built by combining 2D DIW and relaxation of strain.[130] 2D elastomeric polymer precursors were printed on a platform covered with prestretched 2D elastomeric sheets. When the strain of the prestretched sheet was released, the composite buckled into a 3D curvature. In this way, engineers can design and build simple 3D surfaces faster and smoother, such as the flytrap-inspired gripper.

The use of a needle-like nozzle enables precise injection of inks into uncured elastomer matrices. Based on this principle, researchers proposed an embedded 3D (EMB3D) printing method seamlessly integrating soft lithography, molding, and DIW.[131–133] Wehner et al. injected vaporizable inks into a molded elastomer matrix to generate pneumatic networks using the EMB3D method and fabricate the untethered and fully soft robot, octobot.[133] Li et al. proposed a novel EMB3D method to print an elastomer-based soft robot by injecting diluted platinum catalyst ink into a silicone oil matrix.[134] In addition to soft actuators, DIW shows its unique attraction in multifunctional microfluidics fabrication. Su et al. demonstrated a printing strategy by precisely extruding room-temperature vulcanizing (RTV) viscoelastic inks into self-supporting overhanging structures without requiring sacrificial materials and postprocessing.[135] The supporting-free DIW printing is achieved via carefully designed filament stacking orientations and RTV silicone rubber, which could print an overhanging structure with an angle of 37° in the submillimeter regime. Leveraging this approach, a structurally concise microfluidic valve was constructed to regulate the opening and closing of crosschannels through the expansion of air chamber and printed serpentine microfluidic channels integrated with this valve onto the surface of a spherical glass flask.

3.2.2. 4D-Printed Materials and Soft Actuators Based on DIW

In contrast to FFF technology that can only print thermoplastic polymers, which may invalidate and degrade temperature-sensitive components during heating, and VPP which can only print light-curing resins, DIW offers greater diversity in material selection, with options including SMPs, LCEs, hydrogels, and composites. Researchers printed thermoplastic SMPs (like PLA) using the SC-DW method. Incorporating a UV PI into PLA can form crosslinking networks under UV light emitting diode (LED) irradiation to perform SME.[136] Wei et al. mixed PLA pellets, benzophenone (BP), DCM, and Fe_3O_4 nanoparticles to obtain printable SMP ink. Fe_3O_4 nanoparticles endowed the inks with magnetic response, which made them attracted to magnets and capable of acting as an internal heating source under alternating magnetic fields.[137] By printing this material as a planar scaffold and folding it into a spiral scaffold on heating (Figure 4B), the volume of the material at room temperature was limited. By embedding the helical scaffold in a vascular model and stimulating it for 10 s using an alternating magnetic field of 30 Hz, the helical scaffold unfolded owing to SME, which demonstrates the promising application of this material. However, the high glass transition temperature of PLA (T_g: ≈61 °C) limits its applications in the field of minimally invasive medicine.[62] Wan et al. proposed a low-stimulating-temperature SMP (40 °C), named Poly (d,l-lactide-co-trimethylene carbonate) (PLMC) comprising 80 mol% D,L-lactide (DLLA) and 20 mol% trimethylene carbonate (TMC).[138] The response speed of PLMC is affected by the heating temperature. 4D-printed specimen takes 35 s to show complete shape change at 40 °C, but only 0.5 s at 60 °C. Incorporating CNT into PLMC could obtain SMPC ink with electroresponsive shape-changing capability (Figure 4C).[139]

Thermoset SMP ink has garnered significant attention in recent years due to its wide operating temperature range. The most common thermoset polymers used in soft robotic applications are silicone superelastomers such as polydimethylsiloxane (PDMS) and two-component platinum-cured silicones (Smooth-on, USA). Wu et al. incorporated polymer microsphere pore formers into PDMS to print ordered porous structures and enhanced the compressibility of porous elastomers.[140] The recovery rate of the porous SMPC based on this method is significantly affected by compressive strain and heating temperature. Kim et al. mixed microparticles of neodymium–iron–boron (NdFeB) alloy, fused silica nanoparticle (serves as a rheological modifier), and silicone rubber matrix, and then magnetized the composite to saturation under an impulse field (2.7 T) for preparing ferromagnetic domains ink.[141]

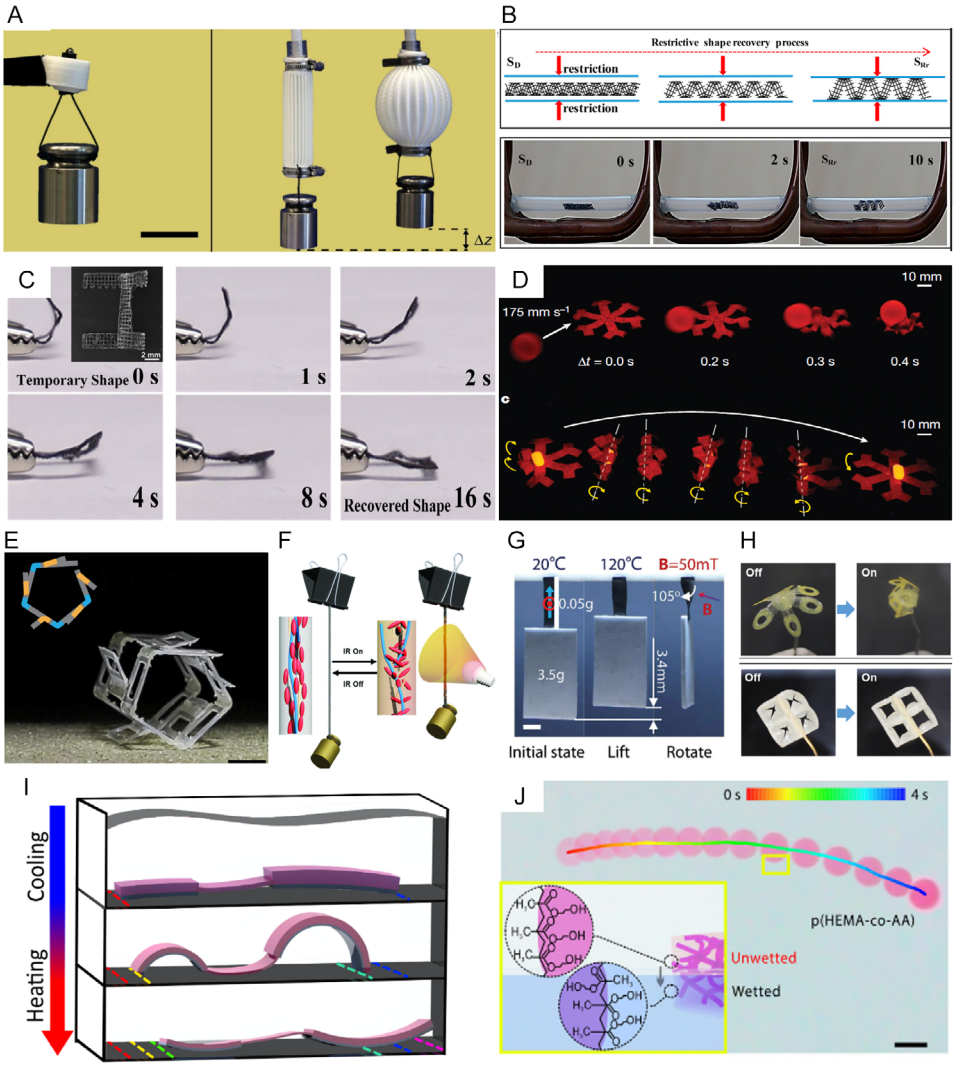

Figure 4. 3D-/4D-printed soft actuators based on DIW. A) Grabbing and contractile SPA made of silicone elastomers with different hardness. Reproduced under terms of the CC-BY license.[127] Copyright 2018, The Authors. Published by Springer Nature. B,C) SMPC printed via DIW. (B) 4D intravascular stents by CPLA/Fe_3O_4 SMPC inks showing remotely actuated and magnetically guidable behaviors. Reproduced with permission.[137] Copyright 2017, ACS. C) Shape recovery process of a folded scaffold made of electroresponsive CNT-based SMPC ink under voltage input. Reproduced with permission.[139] Copyright 2019, Elsevier. D) A hexapedal structure composed of elastomer composite containing ferromagnetic microparticles that could intercept a fast-moving object and roll under a magnetic field. Reproduced with permission.[141] Copyright 2018, Springer Nature. E–H) DIW-printed LCE actuators triggered by heating, irradiating, magnetic, and humidity, respectively. (E) Self-propelling rolling robot with active LCE hinges triggered by temperature change. Reproduced with permission.[144] Copyright 2019, AAAS. (F) Photothermal effect and IR-responsive actuation of LCE/CNT composite filaments. Reproduced under terms of the CC-BY license.[145] Copyright 2020, The Authors. Published by Wiley. (G) magLCE twisting actuator lifting and rotating a weight controlled by temperature and magnetic field. Reproduced with permission.[146] Copyright 2023, Wiley. (H) Reversible h-LCE actuators stimulated by water desorption and absorption. Reproduced with permission.[147] Copyright 2023, Wiley. I,J) Soft hydrogel actuators. (I) Thermoresponsive multi-segmented hydrogel robots with a suspended linker. Reproduced with permission.[149] Copyright 2022, AAAS. (J) Self-powered locomotion of a hydrogel water strider caused by surface tension asymmetry. Reproduced with permission.[150] Copyright 2021, AAAS.

This NdFeB/rubber composite was utilized to design actuators for crawling, rolling, capturing fast-moving objects, and transporting medicines as shown in Figure 4D, showing extremely high driving speeds and energy densities. Silicone-based SMPCs are hyperelastic at room temperature and avoid the limitations of T_g for medical applications. Zhang et al. presented DIW 3D printing of reversible photothermal DA-reactive polyurethanes (PDAPU) based on the Diels–Alder (DA) reaction.[142] PDAPU demonstrates favorable stability, printability, self-healing, recyclability, and SME. Using the DIW printer, PDAPUs can be constructed into complex geometries with infrared (IR) illumination triggering SME behavior.

LCE is a class of shape-changing polymers that can morph reversibly under various stimulations such as heat, light, electric field, magnetic field, and humidity.[143] LCEs consist of anisotropic rigid mesogens and elastic polymer networks

(Figure 3A). Macroscopic deformation of the LCE, such as contraction, is achieved by changing the orientation of the long axes of the mesogens in response to a physical or chemical stimulus, a process called alignment. Thermoresponsive LCEs can be printed into bilayer structures that exhibit orthogonally programmed nematic order and were used to design active hinges.[144] The LCE hinge displays high torque output and can lift loads to 450 times heavier than itself. Figure 4E presents an untethered self-propulsion rolling robot based on the LCE hinge. By incorporating CNT into LCE, enhanced electrical conductivity and photothermal responsiveness can be achieved, rendering them responsive to both electric fields and IR light, see Figure 3B.[145] The artificial muscle fiber consisting of LCE/CNT composite filaments can lift an object 560 times its weight by broadband IR light with $1\,W\,cm^{-2}$ within 28 s (Figure 4F). Electrically driven LCE/CNT composites artificial muscle fibers respond nearly three times faster than photodriven and have higher energy efficiency.

Multiresponse 3D-printed LCEs have also been a hot research topic in recent years. Many LCE deformations require temperature changes generated by Joule heating, photothermal effect, or electromagnetic thermal effect. Some LCEs can respond to multiple stimuli, for example, doping ferromagnetic particles into LCE can respond to three fields (magnetic, electrical, and photo). Sun et al. mixed 5 μm NdFeB into an LCE matrix obtaining a multiresponsiveness composite (called megLCE), which realizes a multimodal morphing response to light and magnetic fields (Figure 3C).[146] When the megLCE was irradiated by a $1\,W\,cm^{-2}$ IR light with a wavelength of 808 nm, it was heated up to 120 °C in 38 s and deformed. The simultaneous application of magnetization and temperature changes to the megLCE produces deformations that are distinct from a single thermal stimulus. Figure 4G illustrates the contraction and twisting of a magLCE strip (0.05 g) prestretched by a 3.5 g object when it was heated and subjected to a magnetic field, respectively. LCE can be responsive to humidity, called humidity-responsive (h-LCE), by activating one LCE surface with an acidic solution to generate cations.[147] Actuation of the h-LCE is realized by the asymmetry of its structure, that is, the activated surface swells in humid environments, while the inactivated surface remains unaffected, which generates a stress gradient to bend. Figure 4H shows h-LCE petals with a 2×2 array of concentric square patterned, which can close under humid conditions and return to the original state upon drying.

Hydrogel is a common material in the design of artificial muscles and bionic robots due to its excellent stretchability, self-healing properties, and biocompatibility (Figure 3A).[148] Similar to the LCEs, hydrogels can be deformed or moved in multiple stimulation modes by adding different functional materials. Pantula et al. used active thermoresponsive poly(N-isopropylacrylamide) (PNIPAM) and passive acrylamide (AAM) to design untethered multisegmented crawling robots (Figure 4I).[149] They designed bending actuators through PNIPAM and AAM and connected two undersized bending actuators through a suspended linker to break symmetry and generate unidirectional motion. Hydrogels were used to design a self-powered water strider robot utilizing the dynamic wetting process to control surface tension asymmetry (Figure 4J).[150] The surface tension of hydrogels changed during water absorption, and the propulsion force of the locomotion changed relatively due to the Marangoni effect. The water strider robot can move for 3.5 h without any external stimulation and can be repeated after drying. Sun et al. doped NdFeB microparticles and nanoclay (as rheology modifier) into microgel-reinforced polyacrylamide (PAAm) hydrogel precursor obtaining magneto-response hydrogel ink. Inspired by arthropods, they designed magnetically actuated flexible joints that can be used to achieve moving, rolling, catching, and releasing. Magnetically driven hydrogel demonstrates its potential for use in robotic surgery.[151] In another study, Luo et al. synthesized biocompatible concentrated alginate/polydopamine (PDA) inks for constructing cell-laden structures.[152] PDA is used as a photothermal agent to generate heat in the absorption of near-infrared (NIR) light, and bilayer structures with an orthogonal pattern based on alginate/PDA ink show self-folding behavior under NIR irradiation.

Excellent material selection is the distinct advantage of DIW, particularly in functional composites. Multiple material printing empowers DIW to fabricate complicated robotic systems incorporating conductive circuits, deformable bodies, sensors, and even variable stiffness areas. In addition, DIW-printed multimodal actuators responding to multiple stimuli deserve to be explored in upcoming studies.

3.3. VPP-Printed Soft Actuators

3.3.1. 3D-Printed Soft Actuators Based on VPP

Flexible photopolymerization resins play a pivotal role in fabricating soft actuators. SLA-based flexible resins are available in a wide range of hardnesses,[153] and SLA-based pneumatic actuators demonstrate good airtightness. Researchers printed pneumatic artificial muscles using flexible resin (Formlabs Flexible 80A) with a hardness similar to TPU (elastic modulus: ≈5 MPa) without any assembly (**Figure 5**A).[154] The artificial muscle shows a high strain of 30%, size scalability spanning one order of magnitude, and high specific contraction force (load capability per unit actuator weight). Inspired by climbing plants, Naselli et al. designed and manufactured a soft continuum robotic arm made of flexible 80A resin.[155] The robotic arm can detect touch force using airtight chambers and helically twine driven by cable. The polyurethane (PU) elastomer can be also used to design soft robotic grippers, robotic arms, and out-pipe robots based on the soft bellow structure.[156] Wallin et al. printed silicone elastomer (elastic modulus <700 kPa) and silicone double networks (SilDNs), using an SLA printer, and demonstrated their application in a soft pneumatic bellow actuator.[157] In contrast to the weak soft–rigid interfaces in FFF printing, the condensation reaction of SilDNs enables cohesive bonding of printed SilDN parts to disparate material surfaces with modulus gradients spanning seven orders of magnitude.

PDMS-based elastomer can be printed via SLA for fluidic elastomer actuator (FEA) design and shows self-healing under sunlight.[158] Yuk et al. demonstrated SLA-printed transparent hydrogel robots by mimicking the tissues and organs of leptocephali. Biomimetic robots were made of PAAm-alginate hydrogels containing more than 90 wt% of water which endows them with optical and sonic camouflaged properties.[159] Mishra et al. designed an autonomic perspiration hydrogel Pneu-net bending

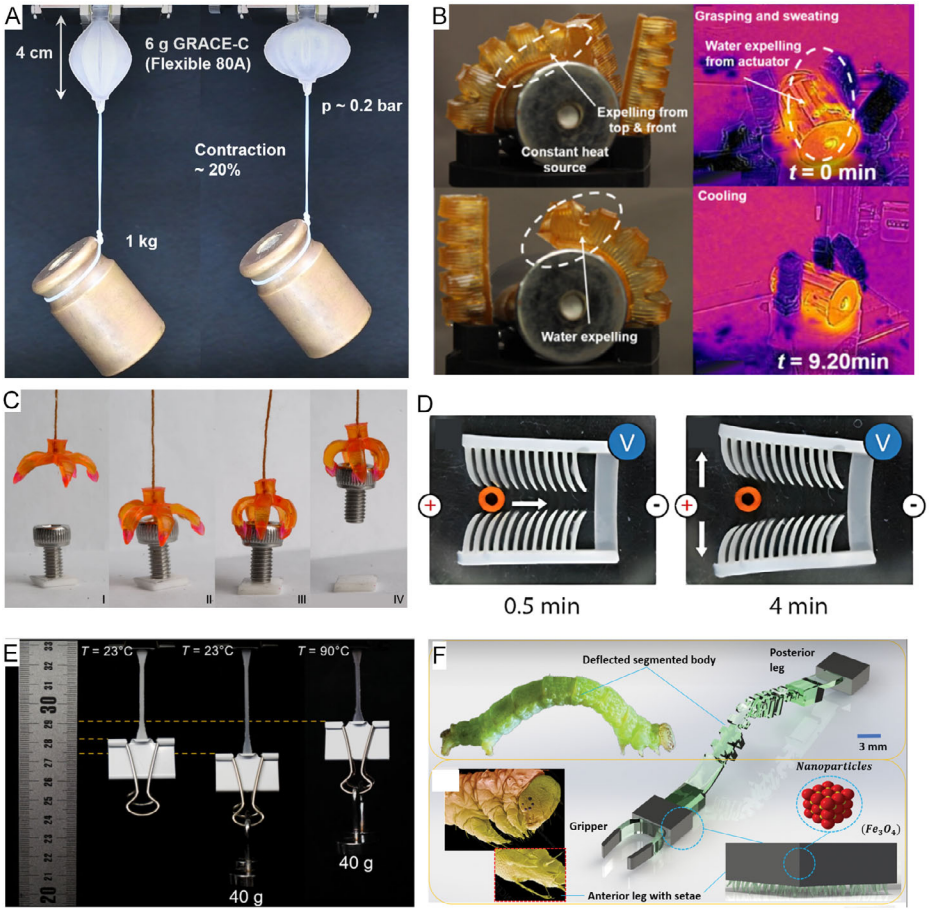

Figure 5. 3D/4D printing soft actuators based on VPP. A) SLA-printed soft pneumatic artificial muscle with high load capability. Reproduced with permission.[154] Copyright 2022, AAAS. B) SLA-printed hydraulically actuated gripper embedded with an autonomic perspiration layer. Reproduced with permission.[160] Copyright 2020, AAAS. C) PμSL-printed multimaterial SMP gripper. Reproduced under terms of the CC-BY license.[163] Copyright 2016, The Authors. Published by Springer Nature. D) DLP-printed EAH transporter consisting of hairs and a bridge with different thicknesses and sequential morphing. Reproduced with permission.[167] Copyright 2018, ACS. E) DLP-printed thermomechanical LCE artificial muscle. Reproduced with permission.[171] Copyright 2021, AAAS. F) Biomimetic soft robot with multimodal locomotion, magnetic-responsive gripper for cargo grasping capability, and multiscale hierarchical spike structures on footpads with features spanning from nanometers to millimeters for slippery environments. Reproduced with permission.[175] Copyright 2021, Mary Ann Liebert Inc.

actuator using a PNIPAM body capped with a microporous (≈200 μm) PAAm dorsal layer (Figure 5B). When the actuator is heated above 30 °C, the PAAm layer expands causing larger pores and ejection of pressurized fluid from the chamber. This perspiration mechanism like human skin can increase cooling speed by 600%.[160]

3.3.2. 4D-Printed Materials and Soft Actuators Based on VPP

SMPs and hydrogels are two smart materials commonly used in VPP due to their diverse actuation mechanism, large deformation, and ease of printing.[32] The traditional resins used in VPP are usually thermoset polymers with high mechanical strength and poor SME properties.[161] The SME of thermoset SMPs is achieved by a two-phase network structure: fixed phase (crosslinking network) and reversible phase.[162] The reversible phase (switching segments) softens when the temperature exceeds T_g, enabling shape morphing. Qi et al. printed methacrylate-based copolymer networks with SME using PμSL and fabricated the Eiffel tower model, cardiovascular stents, and multimaterial gripper based on this material (Figure 5C).[163] The properties of this SMP can be highly tailored by tuning material constituents, including rubbery modulus (1–100 MPa), T_g (−50 to 180 °C), and the failure strain (300%). Triple SMP (TSMP) resins can be fabricated by introducing two temporary shapes with large T_g differences into the resin recipes. Peng et al. configured a TSMP resin and used it to design a microfluidic device with a triple memory effect, which can be used to control the nozzle outputs at three grooves in response to the temperature change.[164] One-way SME, low durability, weak deformation force, and high T_g are still challenges limiting applications of the VPP-printed SMP.

Hydrogel actuation relies on the swelling and deswelling process, which typically has a slow response time and low mechanical strength. Han et al. used PμSL to print Poly(N-isopropylacrylamide) (PNIPAAm) microstructures, a temperature-responsive

hydrogel.[165] The polymer resin composition, light intensity, and PNIPAAm layer thickness would affect the swelling ratio of 3D-printed microstructures. Bending hydrogel actuators achieved by virtual bilayer beams with different swelling characteristics were designed using two different levels of grayscale, and a four-finger gripper was fabricated. Besides, the thermal response temperature of 3D-printed PNIPAAm microstructures is the lower critical solution temperature (typically 32–35 °C) of NIPAAm, which could be adjusted by adding an ionic comonomer. A dumbbell was fabricated with pure PNIPAAm resin on one side and the other side was doped with an ionic comonomer. The dumbbell exhibited TSMP-like characteristics as one side consisting of pure PNIPAAm contracted upon warming to 35 °C, and then the other side also contracted to form a homogeneous structure upon continued warming to 80 °C.

Hydrogels are the most suitable material for humidity-driven soft actuator design due to the swell/deswell effect (Figure 3D). Bilayer hydrophilic/hydrophobic composite structures could bend in response to moisture.[166] The composite structure is made of poly (ethylene glycol) diacrylate (PEGDA) hydrophilic rubber layer attached by a hydrophilic rubber poly (propylene glycol) dimethacrylate (PPGDMA) layer. The bending curvature and response time of the hydrogel actuator can be controlled by adjusting the wall thickness. The bilayer composite can be regulated by the grayscale of the DLP printer. Sequential water-responsive structures can be printed in a single object, like the "S" strap and flower. Han et al. printed electroactive hydrogels (EAH) via PμSL, and the EAH is composed of acrylic acid (AA) monomer and PEGDA crosslinker. This EAH showed bending deformation when it was placed in an electrolyte and applied an electric field (Figure 5D).[167] However, the EAH-based actuator needs to be placed in an electrolyte and is slow to actuate, taking nearly 9 min to open and close a robotic manipulator. Wang et al. reported enzymatically biodegradable soft helical microswimmers made of nontoxic photocrosslinkable hydrogel gelatin methacryloyl (GelMA) printed by a TPP printer.[168] The microswimmer is extremely small with a length of 30 μm and a radius of cylindrical cross section of 1.5 μm, and its magnetism was gained by incubating TPP-printed helical GelMA in aqueous suspensions of Fe_3O_4 nanoparticle. Microswimmers show special swimming behavior in a rotational magnetic field with 8 mT. In addition, the degradation residues of GelMA are not cytotoxic and can serve as dynamic surfaces that support cell adhesion, demonstrating its broad applications in the biomedical field. Except for adhering functional coating onto printed objects' surfaces, introducing functional nanofillers into photocurable resins is still a common way to change resin properties. Zheng et al. fabricated a double-armed microactuator with a size of 26 μm made of PNIPAM/nano-Fe_3O_4 hydrogels, which can bend within 0.033 s under NIR radiation.[169] Fe_3O_4 nanoparticles enable it to be triggered by light and magnetism, and PNIPAM can be thermally driven to contract itself, thus enabling multiresponse.

LCE resins are commonly made of polymerizable mesogens which can be aligned by mechanical stretching, surface alignment, and assisting electric/magnetic fields.[170] Li et al. fabricated a thermomechanical LCE artificial muscle using DLP (Figure 5E).[171] For the DLP-fabricated LCE, the residue resin attached to the bottom of the LCE layer forms an isotropic thin surface layer in the curing process, which causes an asymmetrical cure and the LCE actuator bent rather than contracted when heated to the nematic-to-isotropic phase transition temperature (39 °C). The bending motion can be transformed into a linear contraction by applying load in the direction of shear printing of the DLP-printed LCE actuator. They show the applications of the LCE actuator in untethered crawling, grasping, and weighting. Gold nanorods (AuNRs) can be doped into liquid crystal resins, as an efficient NIR absorber and photothermal agent for light-powered nanocomposite resin.[172] A TPP-printed AuNRs/LCE woodpile structure (140 μm width) with 3 wt% AuNRs elongated 20% under 2 W NIR radiation within 1 s.

Due to the excellent mechanical strength of silicone elastomers, it was widely developed for 4D-printed actuators. Li et al. fabricated an untethered capsule-like robot for drug delivery based on the NdFeB/elastomer composite, and navigation of the microrobot in a maze map was demonstrated, including cargo gripping, transporting, and cargo releasing.[173] A novel VPP strategy was proposed to fabricate programmable magnetic-field responsive materials by controlling the distribution and deposition of magnetic particles using an external magnetic field, named magnetic field-assisted projection SLA (M-PSL).[174] Based on the M-PSL, researchers designed an untethered biomimetic soft robot with spatially varied material compositions, multiscale hierarchical surface structures, and multifunctional components (Figure 5F).[175] During the curing process, an external magnetic field was used to control the distribution of magnetic nanoparticles in a flexible resin (Spot E elastic from Spot A Materials, Barcelona, Spain) to fabricate robust footpads (49 wt% iron oxide particles) and soft body (pure flexible resin). The VPP printer can construct micrometer-sized features, such as 70 μm-long setae-like spikes, on 5 mm-wide robot footpads. The microstructure causes the foot to appear hydrophobic and improves the adhesion of the surface of the robot footpads enabling locomotion in humid environments. Functional structures can be designed on robot footpads, and they designed a magnetically driven gripper to make the inchworm robot carry cargo 30 times its weight.

Printing large-size soft items with high printing speed and high resolution is still a challenge for VPP. VAM is an important and developing printing method with excellent printing speed. The multimaterial VPP with fast speed and high material utilization is still a research gap.

3.4. MJ-Printed Soft Actuators

3.4.1. 3D-Printed Soft Actuators Based on MJ

Despite its low material selectivity, the Polyjet 3D printer is widely used in the design of pneumatic soft robots due to its good shape fidelity, airtightness, and multimaterial printing capabilities. Rubber-like material can be printed for pneumatic bending actuators by reducing the wall thickness in the bending section, forming pseudojoints.[176] Researchers printed pneu-net or bellow actuators via Polyjet, which consists of a rubber-like body (TangoBlack+) for shape morphing and a polypropylene-like male interface (VeroWhite) for quick coupling.[177–179] Soft robots with multiple cavities are complex by casting, requiring a lot of time to wait for the silicone rubber to solidify and a

complex multistep fabrication process. MJ 3D printing allows for one-step forming, showing significant efficiency advantages for small-batch prototyping. They also presented a soft robotic gripper and a soft crawler based on the 3D-printed bellow structure. In addition, Drotman et al. made an omnidirectional actuator by connecting three linear bellow actuators in parallel, which can be utilized for robotic grippers, robotic arms, and robotic legs for quadrupedal robots (**Figure 6**A).[180]

The persistent interface coupling between rigid and soft materials is a vital aspect of robot design, as is the periosteum connection between flexible tendons and rigid bones in the human body. MJ can print soft-rigid hybrid structures, like an anthropomorphic soft skeleton hand with a rigid skeleton and soft ligaments.[181] Saldívar et al. studied the geometrical design of soft–hard interfaces at the voxel level, which is only available in PolyJet 3D printing.[182] Smooth interdigitated connections, compliant gradient transitions, and either decreasing or constraining strain concentrations will improve the robust interfaces avoiding stress concentration. The joining of different hardness materials of similar composition is easy, for example, silicone rubbers with different rigidity. By mimicking squid sucker with rigid ring teeth and a soft teeth-sucker interface, Kumar et al. designed an end effector consisting of a flexible basal plate and rigid tooth-like elements with graded hardness.[183] The junction end of the robotic tooth is soft for robust connecting, and the sharp end is rigid for puncturing, which can smash the eggshell.

Figure 6. Smart structures printed by MJ. A) Quadruped robot with four pneumatic bellow legs. Reproduced with permission.[180] Copyright 2019, IEEE. B) MJ-printed soft robotic hand integrated 18 pneumatic pressure tactile sensors and 15 pneumatic bending actuators. Reproduced with permission.[184] Copyright 2022, IEEE. C) One-shot PolyJet-printed universal gripper based on granular jamming. Reproduced with permission.[186] Copyright 2022, Mary Ann Liebert Inc. D) The slug drive-integrated 14 channels and 28 soft actuators that generate a traveling wave for object transportation. Reproduced under terms of the CC-BY license.[188] Copyright 2020, The Authors. Published by Wiley. E) Reversible self-assembling and disassembling trestle composed of multishape active composites, a rubber matrix integrated with digital SMP fiber layers with different T_g. Reproduced under terms of the CC-BY license.[190] Copyright 2016, The Authors. Published by Springer Nature. F) 4D-printed sequential self-folding box with digital SMP hinges. Reproduced under terms of the CC-BY license.[192] Copyright 2015, The Authors. Published by Springer Nature.

The MJ technique is particularly suitable for building multimaterial structures with complex cavities. Shorthose et al. used a PolyJet 3D printer (J735, Stratasys Ltd, USA) to fabricate a soft robotic hand made of four materials with integrated distributed tactile sensing (Figure 6B).[184] The bending angle of the finger joint actuator driven by vacuum was optimized by embedding a printed rigid central support inside the flexible cavity. Tactile perception is achieved by measuring the internal pressure of air pockets (hardness shore A40) distributed over the phalanges and fingertips. This dexterous robotic hand displays an astonishing DOF and achieves 32 Feix taxonomy grasps and 11 Kapandji thumb opposition poses.

In addition to actuators, MJ printing is widely used in designing functional structures for enhancing robot performance, such as variable stiffness structures. Zhu et al. printed a one-piece variable stiffness SPA by printing a layer jamming bag into the bottom of the pneu-net actuator.[185] The pneu-net body and jamming bag were composed of rubber-like elastomer (Agilus Black, Stratasys, USA) and the jamming layers were made of polypropylene (PP)-like polymer (RGD8530, Stratasys, USA). The granular/particle jamming gripper could be entirely fabricated using a PolyJet printer (Figure 6C).[186] Using the one-shot printing technique, designers unlocked free design, like varying surface patterns, membrane thickness, and granular shape. Zhu et al. designed a rotational jamming layer (RJL) mechanism.[187] Each RJL unit contained two sets of sheets crossed at a rotation axis and enhanced the robotic joint stiffness via vacuuming. RJL was made of PP-like polymer (RGD8530) and constrains the SPA's deformation region.

The properties of multimaterial printing and the wide range of material selection make it feasible to apply MJ printing to fabricate electrically responsive actuators. Schlatter et al. designed electrostatic zipping actuators (Figure 6D) consisting of thin compliant electrodes, dielectric layers, and sacrificial channels using a Jetlab 4 XL printer with nozzles' orifice diameter of 50–80 μm that could pattern materials in two modes (DOD and CIJ).[188] The electrostatic zipping actuators with a similar structure to hydraulically amplified self-healing electrostatic actuators (HASEL) pumping dielectric liquids via voltage-driven Maxwell stress can be used as peristaltic pumps for fluidic systems. Hayes et al. proposed a liquid–solid coprinting MJ printing strategy that can seal liquid in 3D-printed structures as work fluid for FEA.[189]

3.4.2. 4D-Printed Materials and Soft Actuators Based on MJ

PolyJet technology is widely used in the manufacture of SMPCs due to its excellent multimaterial printing capabilities. A laminated SMPC composed of two SMP fiber layers with different T_g (SMP 1: DM9895, T_{g9859}: ≈38 °C; SMP 2: DM8530, T_{g8530}: ≈57 °C) and rubber-like elastomer matrix (TangoBlack+) shows multi-SMEs (Figure 6E).[190] After a single-step thermomechanical (temperature > T_{g8530}) programming procedure, SMP fiber layers were activated sequentially with temperature changes. When temperature exceeds T_{g9859}, the SMPC bends, and when the temperature continues to rise to T_{g8530}, the SMPC returns to its initial state. By changing the arrangement of fiber layers and matrix shape, the multishape active composites were used to design a self-assembling and disassembling trestle, helical actuator, smart hook, and biomimetic insect robot. Multimaterial printing SMPCs can be used for the rapid transition from 2D plates/rods/fibers to 3D structures to save 70–90% printing time and materials compared with direct printing.[191] The printed 2D SMPCs consist of a SMP layer (Vero) and an elastomer layer (Tango+). In the printing process, compressive stress is stored in the elastomer layer but not in the SMP layer. When $T > T_g$, the SMP layer softens, and the elastomer layer extends to bend the SMP layer. By designing the pattern, the composite rod and planar mesh with a hexagonal pattern can be transferred to a helical spring shape, cubic frame, buckyball, etc. By mixing different inks during the jetting process, it is possible to synthesize SMP with different mechanical properties and T_g, named digital SMP. Mao et al. printed sequential self-folding structures using digital SMP, which can fabricate seven digital SMP flexible joints at once (Figure 6F).[192]

LCEs can be printed as actuators via inkjet printing technology.[193] Artificial cilia (10 μm thick, 3 mm wide, and 10 mm long) have been fabricated and can bend under visible or UV irradiation, making them suitable for use as mixers or pumps in microfluidic systems. In principle, the fabrication of LCEs and hydrogels using MJ is theoretically possible.

Pioneer researchers used MJ to print hydrogel for cell-laden structures but encountered limitations such as low throughput and single-material printing.[194–196] However, there is limited research focused on manufacturing LCE or hydrogel actuators via MJ printing, which might be caused by costly MJ printers with precise closed-loop feedback control leading to customizing the print material difficultly.[197] Potential soft robot applications of 4D print LCE or hydrogel-based MJ printing are worth exploring owing to the multimaterial, high print speed, and high-resolution features.

3.5. SLS-Printed Soft Actuators

3.5.1. 3D-Printed Soft Actuators Based on SLS

SLS is a common process for designing SPAs because of its ability to print TPU materials. Scharff et al. designed a robotic hand composed of four sections: a bellow-type bending actuator for fingers, a helical twisting actuator for the robotic wrist, a bidirectional actuator for enhancing palm stiffness, and sensing air chambers for palm contact feedback.[198] The human-sized robotic hand was printed using TPU 92A material via SLS monolithic molding in 12.5 h. Based on the bellow-type actuator, Du et al. proposed a robust soft worm-like crawling robot that can climb on flat ground, slopes, and vertical walls.[199] Guo et al. printed a ball joint using polyamide−12 (PA12) by SLS. By assembling the joint with a soft extending actuator, the joint stiffness could be adjusted by inflating the actuator to exert pressure on the ball surface.[200] A structured fabric skin was printed with nylon via SLS but shows fabric-like flexibility due to the chainmail geometry.[201] By adjusting the unit cell structure of the chainmail skin, it can be programmed to stretchable or nonstretchable structures. By winding the chainmail skin to a cylinder elastomer bladder, bending/extending/expanding actuators were designed.

3.5.2. 4D-Printed Soft Actuators Based on SLS

Similar to FFF, the thermoplastic SMPs can be used for SLS powder. Mei et al. synthesized a thermoplastic polyamide elastomer (TPAE) with SME. A flower and helical spring were printed via SLS using the TPAE.[202] A novel TPAE with reversible two-way SME was synthesized using a two-step method that did not require additional multimaterial composite structures.[203] Mechanical programming of two-way TPAE can be accomplished by applying an external force only during the first heating process. After programming, the two-way TPAE enables reversible deformation between the printed shape and the programmed position controlled by heating and cooling. A bending actuator was designed to show the two-way SME of the TPAE.

Magnetic-responsive TPU composite can be printed by mixing magnetic $Nd_2Fe_{14}B$ powder and TPU powder.[204] Researchers fabricated an untethered soft robotic gripper with this composite via SLS, and the grasping/releasing of the gripper was controlled by the magnetic field. Ouyang et al. synthesized a polyurethane containing reversible DA bond (PUDA) covalent adaptable network for SLS printing.[205] By incorporating CNT, the PUDA/CNT composite shows functions of self-healing and SME that can be triggered by heating or NIR irradiation. A Miura origami structure was fabricated that can be flattened during heating and recovered to the initial folded state under reheating. In addition, a simple composite circuit was printed, and the LED could be remotely controlled by NIR light. Blending functional nano-/microparticles (like graphene) and basic powders (like TPU) can be used to fabricate polymer composite for conductive polymers or sensor design.[206,207] The CNT/PDMS composite printed by SLS was applied as a strain sensor.[208]

Overall, the publications about SLS-based soft actuators are far fewer than other 3D printing methods due to high cost, limited materials, mediocre resolution, and poor multimaterial printing capability.

3.6. Conclusion of the 3D-Printed Actuators

For the soft actuators based on the nonfunctional materials, TPU, and silicone elastomer, most of them can be directly printed at once, like passive deformation structures (e.g., fin ray structure), groove for tendon-driven actuation, bellow-type FEA, vacuum-driven suction cap, granular/particle jamming bag, etc. Soft actuators based on single-functional materials or composites (SMPs/hydrogels/LCEs or their composites reinforced by CNT/Fe_3O_4/graphene nanoparticles) were commonly manufactured via DIW or VPP. The actuation of those smart materials/composites could be triggered by temperature/light/magnetic/humidity/ultrasound/electricity/chemical solutions decided by the matrix and functional particles of composites. At the current stage, 3D-printed smart materials (hydrogels and LCEs, etc.) are mostly simple demonstrations, like a bending strip actuator or contractile artificial muscle, the future trend should be to integrate them into robotic systems.

However, there are numerous actuators composed of multiple materials with different properties, and their fabrications are more complicated, especially for EAPs with layered composites, such as dielectric elastomer actuators (DEA), ionic polymer–metal composite (IPMC), and HASEL actuators. For better mechanical performance or more efficient fabrication, engineers used 3D printers to build actuator components and then create the complex structure of the actuator in subsequent fabrication via bonding, casting, electroplating, chemical treatment, etc. DEA consists of an elastomer sandwiched by two conductive electrodes, which could deform and generate actuation force by applying a high electric field (usually takes a few thousand volts) due to Maxwell stress. Researchers printed 3D electrodes for DEA design via DIW and manually encapsulated them in an insulating dielectric matrix by casting.[209] Despite the sandwich structure of the IPMC, which is similar to that of the DEA, the working principle and mechanical performance are vastly diverse. The working principle of IPMC is ionic migration, which can be triggered under a relatively low voltage and generate a visible deformation.[210] Carrico et al. extruded a thermoplastic Nafion precursor filament and printed Nafion membranes via FFF.[211] Then, the Nafion membrane undergoes a chemical functionalization process to hydrolyze the membrane and render it electroactive. Finally, metal electrodes were attached to the membrane by an electroless plating process to acquire the IPMC actuator. HASEL actuators incorporate the advantages of DEA and FEA and solve their limitations, which use both electrostatic and hydraulic forces to generate high strain, fast response, high energy density, and self-sensing Peano actuation.[212–214] O'Neill et al. fabricated a tough silicone-urethane bellow structure via CLIP printing first.[215] Then, they painted conductive silver onto the inner surface of a flexible substrate and attached the substrate to the actuator using silicone–urethane resin. Finally, hydrogel precursor solution was injected into the cavity of the actuator to complete the HASEL actuator fabrication.

Multimaterial 3D printing techniques, such as FFF, DIW, and MJ, enable the creation of complex robotic systems in a single step. For systems composed of multiple materials with different properties, researchers often print distinct components using appropriate 3D printing principles and subsequently assemble them. Zhang et al. designed a bending actuator with a flexible pneu-net chamber, cooling channel, SMP variable stiffness layers, and heating circuit.[216] The main body of the bending actuator, cooling channel, and SMP layers were printed via MJ, while the heating circuit was fabricated by DIW using silver nanoparticle ink. After printing, the four sections were bonded together. One reason for this step-by-step printing may be the limited selection of materials available for the PolyJet printer. Multistep printing also avoids complex support for better print accuracy and saving postprocessing time.

Differences in material selection, print resolution, forming area, and print speed between printing methods also dictate that different processes are necessary to produce different parts in some cases. **Table 1** summarizes and compares the key specifications of different printing techniques such as precursor material properties, printable soft polymers, printing speed, maximum resolution, support requirements, advantages, and disadvantages. Inspired by gecko microfibers, gecko adhesion (dry adhesion) was proposed for gripper design as a versatile functional structure, which bears tangential loads through the Van der Waals forces generated between the fibrous nanostructures and the object surface.[217] In previous work, the load-carrying capacity of the gripper could be significantly improved

Table 1. Capabilities of different 3D printing mechanisms. The number of stars represents the building speed, where more stars indicate a faster speed.

	FDM	DIW	VPP	MJ	SLS
Precursor materials	Thermoplastic polymer filaments	Curable pseudoplastic inks	Photopolymers resins	Low-viscosity polymer inks	Thermoplastic polymers powders
Typical soft polymers	TPU/SMP	TPU/Elastomer/hydrogel/LCE/Composites	TPU/Elastomer/hydrogel	TPU/Elastomer	TPU/SMP
Build speed	****	*****[323]	******(VAM)[67]	***	****
Maximum resolution	≤78 μm[99]	≤50 μm[249]	≤100 nm (TPP)[324]	≤10 μm[325]	≤100 μm[11]
Support	Water-soluble material/Standard filaments	Water-soluble material	Standard resins	Wax support/Water or chemical-soluble material	Not required
Pros	1. Low cost 2. Easy maintenance 3. Multimaterial printability	1. Excellent material selectivity 2. Multimaterial printability	1. High resolution 2. High printing speed 3. Great surface finish	1. Excellent multimaterial printability	1. No support 2. Large build volume 3. High mechanical properties
Cons	1. Limited thermoplastic materials 2. Anisotropic mechanical properties 3. Poor resolution	1. Limited forming area 2. Poor resolution	1. Complex post process 2. Poor multimaterial printability 3. Biotoxicity of most resins	1. Complex post process 2. High equipment and maintenance cost 3. Limited materials	1. Poor material selectivity 2. Poor multimaterial printability 3. Health hazard 4. Rough surface

by adding a gecko adhesion layer with micrometer-scale features on the contact surface of the gripper.[218] There are studies on printing gecko adhesion layers with superhydrophobicity by TPP and DLP techniques, but no research has yet explored 3D-printed robots with gecko adhesion layers printed in a single step.[219,220] The main reason is that molding this microscale structure leads to prolonged printing speeds. In addition, VPP-based printing has extremely poor multimaterial printing capability, and the material used in the active actuation section is different from that of the gecko adhesion layer. Using VPP to print flexible materials in different positions with different printing accuracies can optimize the printing time while obtaining local high-precision hierarchical structure. One-piece molding of SPAs with a gecko adhesion layer is a worthwhile research point in the future.

4. Applications of 3D-Printed Soft Robots

Prominent deformation, exceptional mechanical performance, and diverse soft actuation methods have inspired engineers to design unprecedented devices. Soft robots have demonstrated amazing adaptability for industrial applications, with their compliant structure showing amazing adaptability when interacting with fragile objects and complex environments. Moreover, these biologically inspired soft actuators can mimic biological characteristics that can be utilized to make robots better suited for specific applications. The emergence of soft robots may break the setting of workplace robotics safety for robotic arms, allowing robots to be more safely integrated into the user's daily life due to their intrinsic flexibility of the soft body reducing dependence on sophisticated sensors, light-sensitive vision systems, and complex algorithms. For some specific applications, such as wearables and haptic feedback, safety is the most critical consideration for users. Herein, we discuss 3D-printed soft robots for diverse applications including grippers, artificial muscles, locomotion robots, biomedical devices, and embedded sensors (**Figure 7**).

4.1. Grippers

Robotic grasping and manipulation are essential functions that enable robots to interact with external environments, like end effectors in surgical robots, soft grippers in harvesting robots, underwater manipulators in remotely operated vehicles, and robotic hands in humanoid robots, etc. 3DP is the most effective fabrication process for soft grippers with complex chambers. In general, flexible grippers can be divided into three categories according to the actuation mechanisms: 1. by actuation, 2. by controlled stiffness, 3. by adhesion, as illustrated in **Figure 8**A.[221]

Different actuation principles excel in specific applications, and selecting the appropriate gripper designs can significantly improve grasping performance. We categorize the ease of object manipulation by different gripper working mechanisms into four levels (Figure 8B), ranging from easy to difficult: Level 1: The actuation principle allows the gripper to manipulate the object easily and robustly. For instance, an electroadhesion gripper can effortlessly grasp a playing card and adjust its orientation as needed. Level 2: The gripper can grasp the object using this actuation principle, but the gripper's attitude needs to be adjusted or restricted. For example, a FEA gripper can grasp a small nut, but the operator is required to align the gripper tip with the nut due to the wide grasping range of the FEA gripper. Level 3: Using this type of gripper to manipulate the object requires the assistance of sensors to prevent damage to the object. For instance, a fin ray gripper can grasp bread, but without a sensor, it may squeeze the bread. Level 4: This actuation method is unsuitable for grasping this object type. To illustrate, a gripper based on SMP will deform or even destroy soft targets

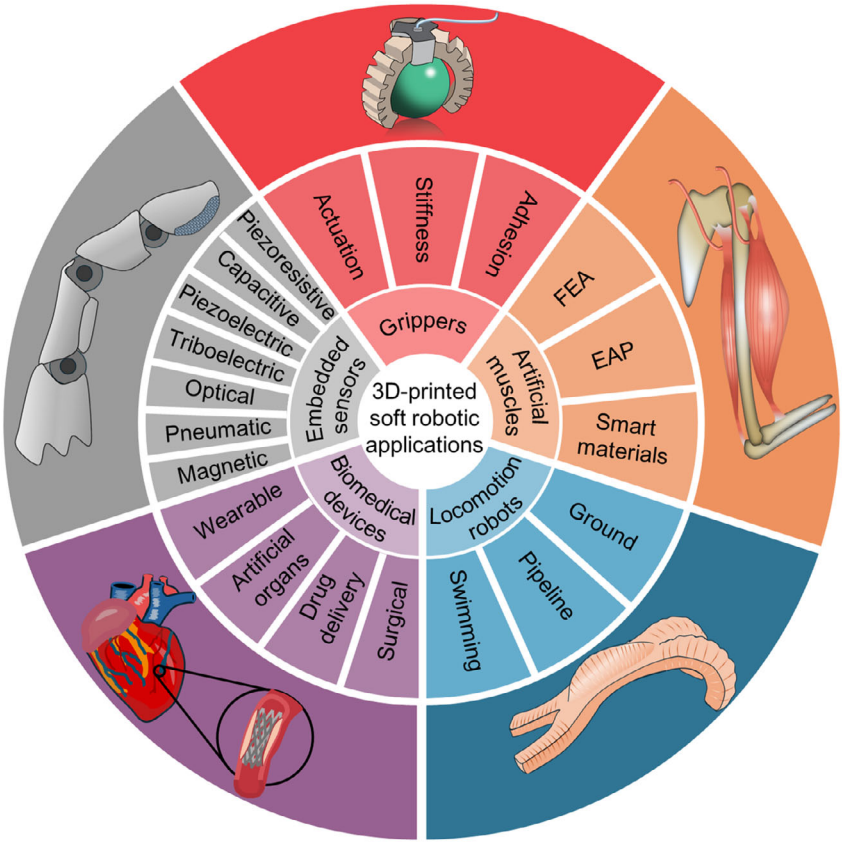

Figure 7. Applications of 3D-/4D-printed soft actuators in the fields of grippers, artificial muscles, locomotion robots, biomedical devices, and embedded sensors.

causing failed grasping, as a large nominal stress is required for SMP deformation. In addition, the universal gripper based on granular jamming cannot grasp sharp objects, as they may puncture the gripper's elastic film. More detailed properties of the soft gripper based on diverse working principles were discussed in Shintakes's work.[221]

Soft grippers based on direct actuation using passive structures, SPAs, and stimuli-responsive materials are versatile designs in various fields. All passive structures used for soft grippers can be 3D printed. Researchers used flexible materials to design passive structures that could generate shape morphing upon contact with targets, such as fin ray grippers, bistable origami structures, self-adaptive foam materials, etc.[222–225] In addition, due to the high specific lifting weight (object mass/gripper mass), Krigami and woven structures have been explored for ingenious gripping of small objects.[226–228] Inspired by human fingers, tendon-driven soft fingers with rigid or flexible joints represent another common passive structure design.[229] There are two main design strategies for 3D-printed SPAs. One is the pneu-net or bellow-type bending or extending actuators.[107,224] A vacuum-driven 3D-printed groove with a closed chamber can also produce deformation similar to the tendon-driven actuator.[184,230]

Smart materials are widely used for gripper designs responding to diverse stimuli. LCEs and hydrogels are common groups of materials that deform under heating. Thermal-controlled soft grippers based on pure LCEs/hydrogels were widely printed for small-scale grasping.[171,231] Except for LCE/hydrogel composites based on the photothermal effect, liquid metal polymer composites (LMPCs) can be used to design soft grippers via SLA.[32,232,233] Magnetic-responsive grippers were generally achieved by soft elastomers blended with ferromagnetic particles.[173] Son et al. presented a multiresponsive gripper made of ultrasound-responsive NIPAM-based gel, stimuli nonresponsive structural AAm-based gel, and magnetic-responsive ferrogel.[234] The grasping and releasing of the gripper is triggered by ultrasound (Figure 3E), and the locomotion is controlled by magnetic field without the need for decoupling of the two functions. Humidity-responsive LCEs/hydrogels can also be used to design soft grippers, though the practicability is limited by terrible control and low response time.[147] EAP requires more steps to fabricate complicated structures rather than only 3D printing. Tyagi et al. designed a microscale EAP gripper, with polypyrrole (Ppy)/hydrogel/gold sandwich structure, for soft microrobots (400 μm × 3000 μm × 25 μm).[235] The gripper can grasp with a maximum frequency of 1 Hz under 1 V voltage input. DEA-based soft grippers could be fabricated by printing TPU on a prestretched dielectric elastomer membrane coating with electrodes.[236] The DEA gripper keeps grasping gesture at the initial state and opens by applying a 5 kV voltage.

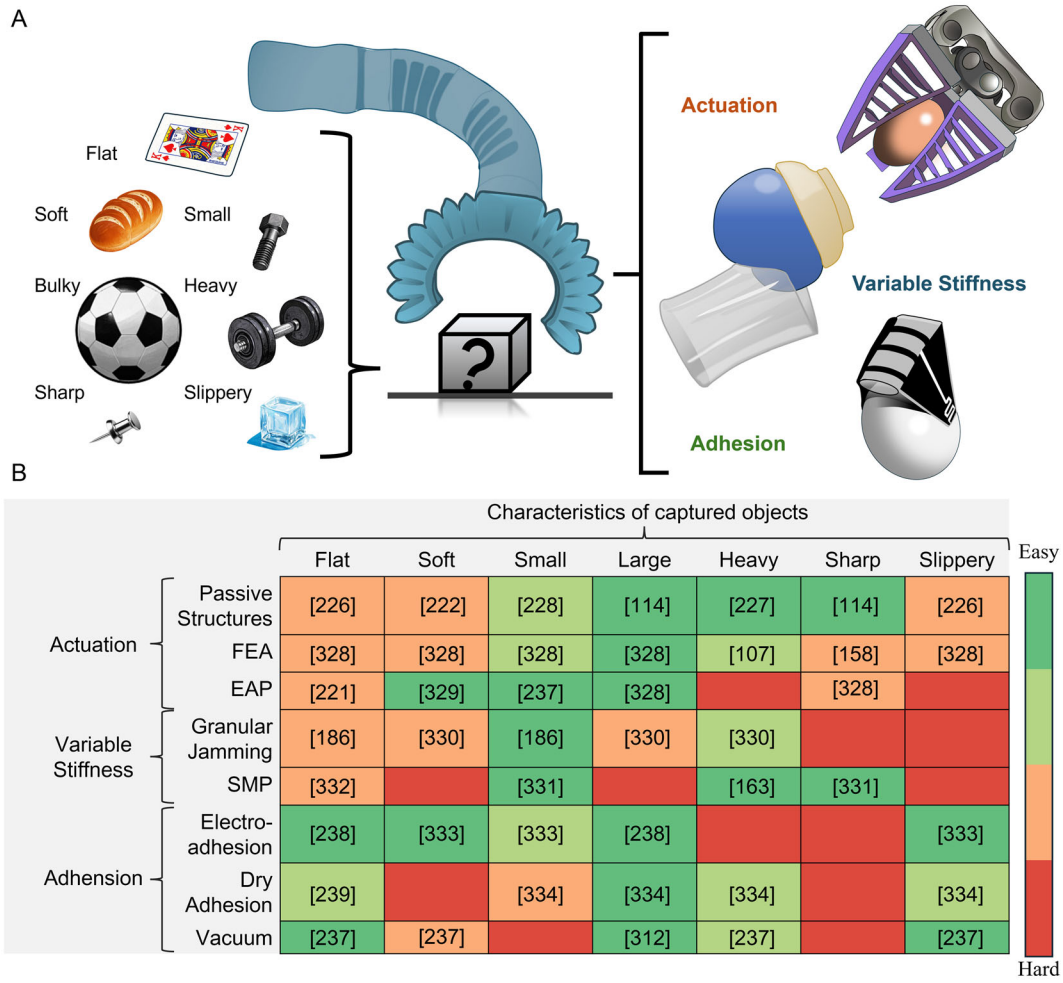

Figure 8. 3D-printed robotic grippers in unstructured environments. A) Soft robotic gripper facing diverse grasping requirements. B) Performance of the soft gripper when grasping objects with different properties. Common EAP grippers are based on DEA, IPMC, and HASEL actuators.

Variable stiffness mechanisms are widely used in robotic gripper design due to their universal adaptability. Howard made a gripper based on particle jamming via PolyJet.[186] In addition, SMP-based soft grippers show excellent variable stiffness capability and can lift objects far heavier than themselves. Although most 3D-printed SMPs exhibit only one-way SME, Li's work shows a recipe for two-way TPAE SMP and might be further extended to other printing methods like FFF.[203]

Soft grippers based on adhesion can be classified as vacuum suction, electroadhesion, and gecko adhesion. Koivikko et al. designed a suction gripper with an elastomer film via VPP.[237] The main body and film of the suction were made of rubber-like elastomer with shore 35A, and the suction shows better grasping capabilities in catching small and fragile objects compared to commercial suctions. Xiang et al. printed flexible electroadhesion pads via FFF using PLA and CPLA.[238] Although the PLA can slightly bend by designing into a thin sheet, the flexibility is far less than TPU or rubber elastomer. DIW can print conductive inks in elastomer substrate for more flexible electroadhesion pad design, and one-shot printing of grippers based on other actuation mechanisms (like SPA) combined with electroadhesion pads will be an interesting topic. Additionally, studies have explored the fabrication of gecko-inspired microstructure to achieve superhydrophobicity, enhancing adhesion performance.[218,219]

The application of the VPP-printed gecko-inspired microstructures for grasping enhancement and one-shot printing of grippers incorporating these structures warrants further investigation. A hybrid gripper could combine the advantages of these actuation mechanisms, and one-shot 3D printing of the hybrid gripper is a valuable research topic. Although soft grippers can adapt to diverse objects, tactile sensors and deformation sensors are required for grasping fragile objects, like tofu and raspberry. Sensor-integrated soft gripper based on multi-material 3DP is a promising area.

4.2. Artificial Muscle

Artificial muscles inspired by nature show high compliance and are widely applicable in soft actuation for humanoid robots, bio-inspired robots, wearable robots, etc. Based on the actuation

mechanisms, the 3D-printed artificial muscle can be classified into FEAs, EAPs, and smart materials.[239]

FEAs were commonly used in artificial muscle or contracting actuator design. A straightforward example of 3D-printed artificial muscle is designed relying on structural shrinkage like TPU bellow, which contracts under negative pressure.[240] Besides, laterally buckling on a nonstretchable constraining layer leads to contraction deformation, like McKibben muscle,[241] fiber-reinforce contractile actuator,[127] and diamond-shaped band actuated by an extending bellow.[101] Soft pneumatic helical actuators can be used to actuate joint rotation like a muscle, and the helical pneu-net structure can be printed via FFF.[242,243]

Researchers have explored the use of SMPs to design artificial muscles.[244] Prestretched 3D-printed one-way SMP contracts when the temperature is higher than T_g. The softening of SMP at high temperatures limits its load-bearing capacity. SMP is currently suitable for microscopic, lightweight, and low-driving frequency robotic actuation. Although SLM-printed NiTi-based shape memory alloy (SMA) was widely studied,[245] and SMA coil can be used in tendon-driven structures as artificial muscle,[246] there is no 3D-printed SMA for artificial muscle design due to high costs of equipment and material. However, 3D printing is an important way to fabricate SMA with complex structures, because nitinol is hard to weld.

DEA was widely used in underwater robots, crawling robots, flying robots, and robotic hands as artificial muscles due to fast actuation response, large deformation, and high energy density.[247] Both electrodes and dielectric elastomer could be printed via DIW, and the 3D-printed DEA is not restricted to traditional sandwich structures.[248] HASEL artificial muscle has a similar structure to DEA, which has larger strain and a softer body.[213,249] Hydrogels and LCEs were common choices for artificial muscle design, and they can be printed to various shapes via DIW. Notably, material coextrusion and subvoxel control DIW enables flexible material design for hydrogel and LCE, which could be used to build composites with programmable structures.[59] Besides, twisting string actuators (TSA) and piezoelectric actuators can be used as artificial muscles but are not suitable to be fabricated by 3D printing.[239]

Currently, artificial muscles show superior performance compared to natural muscles, such as working frequency,[209] strain,[101] work capability, and power density.[250] Nonetheless, different types of artificial muscles can only surpass natural muscles in certain aspects. Designing and fabricating artificial muscles with a long lifetime, compact structure, self-healing, high strain, large force, fast response, and easy actuation are still challenges.

4.3. Locomotion Robots

Locomotion robots play a vital role in exploring hazardous environments like patrolling, postdisaster rescue, deep-sea exploration, etc. According to the working environment, locomotion robots can be categorized into ground robots, in-pipe robots, out-pipe robots, swimming robots, and flying robots according to application scenarios.

Soft crawling robots can locomote on the ground based on diverse gaits, like multilegged robots, creeping robots, rolling robots, etc. A hexapod robot composed of soft bellow actuators, a rigid frame, and complex air chambers was fully built via vision-controlled MJ (**Figure 9**A).[251] 3D-printed multilegged robots are suitable for multiterrain locomotion with good loading capacity and orientation control. Inspired by caterpillars, earthworms, and inchworms, researchers developed numerous creeping robots. The deformation of creepers was achieved by pressure-controlled bellow contraction (Figure 9B) or TSA/SMA-driven adaptive body flexion,[252–254] and the locomotion stroke was decided by the frictional differences between the front and rear feet via adhesion (electric or vacuum) or passive structures (multimaterial or high friction structure).[255,256] Generally, soft crawling robots have relatively simple structures, small profiles, poor steering, terrible off-road capability, low locomotion efficiency, etc. One strategy for the soft rolling robot is to use a stick actuator with multisection asymmetric deformation, which has high speed but limited controllability.[257,258] In addition, soft rolling robots can be made of a circle or polygon frame, actuated by circumferentially arranged actuators. The actuators for rolling locomotion could be any actuator with visible deformation like, thermal-responsive LCE,[144] DEA,[259] and SPA.[260] However, current studies focus only on 2D rolling robots limiting their steering, and 3D-printed soft rolling robots with polyhedron structures deserve to be investigated in the future.

Inspection, maintenance, and repair of pipes are labor intensive and dangerous tasks. The soft in-pipe robot can easily maneuver through complex pipe chambers (slopes, sharp bends, and junctions) and adapt to pipes with different diameters. Most in-pipe robots were inspired by worms with expansible ends and an extensible body.[261] Lin et al. proposed a novel in-pipe robot with only one McKibben muscle as an actuator, as shown in Figure 9D, and the robot propelling was achieved by 3D-printed elastic ribbons that could change the friction of the front and rear of the robot during muscle contraction.[262] The design philosophy of the soft out-pipe robots is similar, typically consisting of two grasping mechanisms and one extending actuator. Xie et al. optimized the pneu-net actuator using nontensile material and designed an out-pipe robot with two grippers and an extensible body that could lift a weight of 1 kg (Figure 9C).[263]

Inspired by aquatic creatures, researchers focus on soft swimming robots for environmental exploration and monitoring. Matharu et al. printed a TPU jellyfish frame and the swimming stroke was controlled via SMP.[264] MJ has been used to create soft–rigid hybrid components for robotic fish, ensuring that the soft sections remain watertight during deformation.[265] A water strider robot floating on water can be driven by a small shear force.[150,266] Amphibious bionic robots eliciting multienvironmental adaptations show promising research prospects, like tortoise robots and frog robots.[267,268] The membrane structure and lightweight hollow structure manufactured by 3D printing were studied for flying robots,[269,270] but the 3D-printed actuator for flying robots is still blank. Untethered design is the most important factor for all soft locomotion robots in practical applications.

4.4. Biomedical Devices

This section summarizes 3D printing actuator applications in biomedical engineering, like wearable robots, artificial organs, drug delivery, and surgical robots.

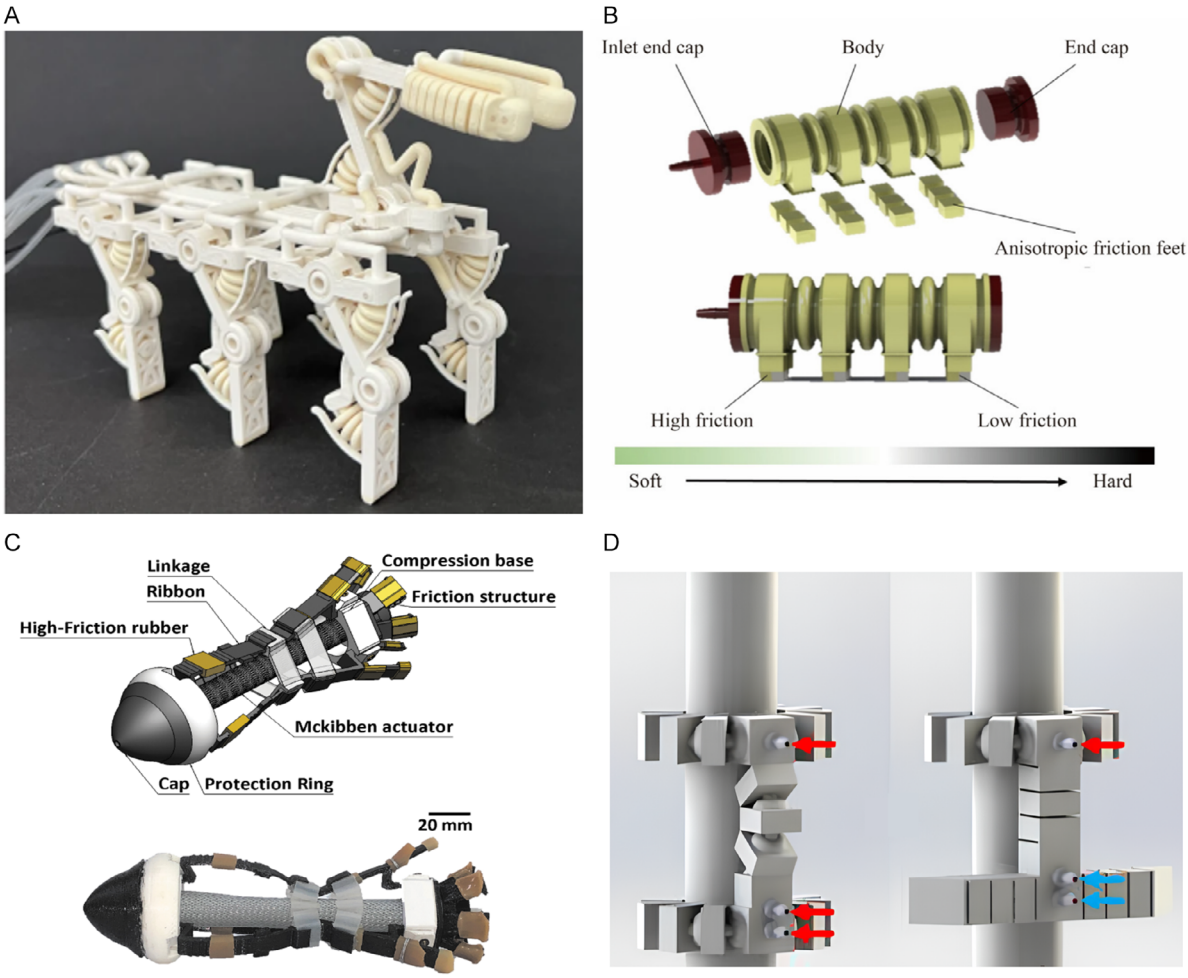

Figure 9. 3D-printed soft locomotion robots for various scenarios. A) MJ-printed hexapod robot consisting of rigid skeletons and flexible bellow actuators. Reproduced under terms of the CC-BY license.[251] Copyright 2023, The Authors. Published by Springer Nature. B) PolyJet-printed caterpillar-inspired crawling robot based on multimaterial anisotropic friction feet. Reproduced with permission.[252] Copyright 2020, Elsevier. C) In-pipe crawling robot with a single Mckibben actuator and 3D-printed elastic ribbons for enhancing anisotropic friction. Reproduced with permission.[262] Copyright 2023, Mary Ann Liebert Inc. D) FFF-printed inchworm-inspired out-pipe robot. Reproduced with permission.[263] Copyright 2021, IEEE.

Wearable or assistive robots help patients with functional disability to assist rehabilitation training or improve their quality of life. The finger flexion and extension of the human hand can be assisted by a tendon-driven actuator or soft bending actuator. The tendon anchoring support or SPA on the dorsal hand can be 3D printed for easy customization (**Figure 10**A).[271] Xia et al. proposed a novel passive bellow actuator (PBA) for robotic gloves.[272] PBA laid on the dorsal finger could help finger extension when pulling the bellow using a tendon, and PBA can assist finger flexion using the elasticity of TPU material when releasing the tendon. The PBA combines the comfort of SPA and the fast response of tendon-driven robots, not relying on an airtight bellow structure. A vacuum origami actuator with compact size can be deployed on the face to treat facial paralysis (Figure 10B).[273]

Patients with organ failure or even removal due to disease or accident rely on medical intervention devices, prostheses, or artificial organs to enhance or compensate for the corresponding functions. The application of 3D-printed cardiac stents and tracheal stents with biocompatibility, in vivo degradation, SME, and good mechanical properties has been widely investigated (Figure 1C).[123] However, there is still a long way to go for clinical trials.[274,275] 3D printing is widely used in prosthetic hand fabrication avoiding high-cost mold manufacturing.[276] Flexible gripping reduces the sensing and control requirements of the prosthetic hand, while a compliant human–robot interface ensures wearing comfort and safety. Bioprinting scaffold with biocompatibility for cell and tissue culture is a future research hot point.[277]

Magnetic navigation is a safe, untethered, high-DOF, penetrable actuation strategy for drug delivery using micro/nanorobots (Figure 10D).[173] 3D-printed hydrogel carriers derived from biological tissues (like gelatin) are biologically friendly by adding magnetic particles to enable them to navigate through convoluted and multibranched blood vessels.[278] Drug release can be triggered by noninvasive stimuli such as oscillating magnetic fields, ultrasound signals, light, and pH, and these stimulus-responsive delicate structures can be printed by DIW (Figure 10E).[234,279–281] This targeted drug delivery improves

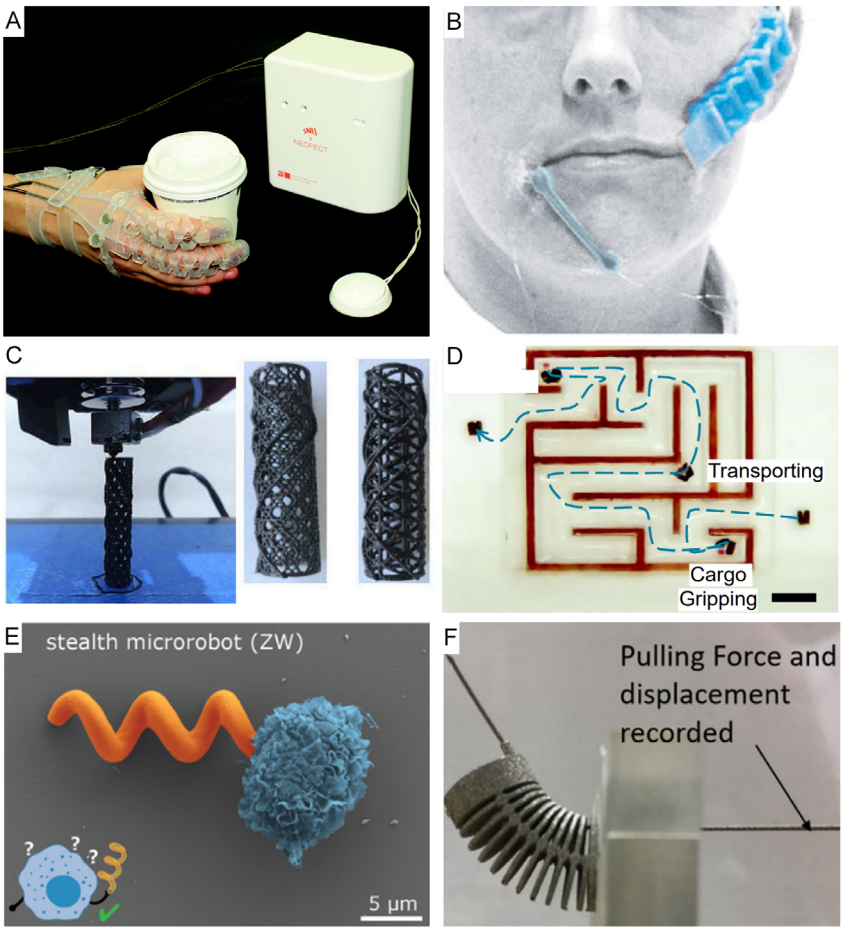

Figure 10. 3D-printed biomedical robots for wearable devices, implantable medical devices, drug delivery, and surgical robots. A) FFF-printed TPU antagonistic tendon routing system for hand rehabilitation after spinal cord injury. Reproduced with permission.[271] Copyright 2019, Mary Ann Liebert Inc. B) Contractile actuator compensating smiling muscles for facial rehabilitation after facial paralysis. Reproduced with permission.[273] Copyright 2022, Mary Ann Liebert Inc. C) FFF-printed tracheal scaffold mimicking porous glass sponge actuated by a magnetic field. Reproduced with permission.[123] Copyright 2019, Elsevier. D) DLP-printed magnetic miniature capsule soft robots achieving cargo gripping, transporting, and releasing. Reproduced under terms of the CC-BY license.[173] Copyright 2023, The Authors. Published by Wiley. E) TPP-printed nonimmunogenic stealth hydrogel microrobots for magnetic-driven drug delivery and avoiding detection by macrophage cells. Reproduced under terms of the CC-BY license.[281] Copyright 2020, The Authors. Published by Wiley. F) SLM-printed tendon-driven stainless steel flexible joints for snake-like surgical instruments. Reproduced with permission.[284] Copyright 2019, IEEE.

the precision of the drug's location and dosage, avoiding further harm from overdosing and invasive procedures. Capsule endoscope with magnetic navigation is a promising protocol for gastrointestinal biopsies.[282]

Endoscopic surgery is performed through small incisions or natural orifices into the insufflated abdomen using a continuum robotic guidance, endoscopic imaging, and high-precision manipulators.[283] Rigid mechanical coupling and cable-driven actuation ensure surgical precision, and the flexible joint mechanism can be manufactured by 3D printing (Figure 10F).[284] FEA-based continuum robots were used as robotic arms for surgical robots, but their development was limited by miniaturization and nonlinear control.[285,286] Despite these advancements, 3D-printed biomedical devices remain far from clinical testing due to limitations in actuation performance, control precision, lifespan, and biocompatibility.

4.5. Embedded Sensors

Multimaterial printing (FFF, DIW, MJ) allows sensors and actuators to be integrated in a single step without cumbersome assembly. Based on the working mechanism, 3D-printed soft sensors can be categorized into piezoresistive sensors, capacitive sensors, piezoelectric, triboelectric sensors, optical sensors, pneumatic pressure sensors, and magnetic sensors.[287,288] Sensors for soft robots require both proprioception to sense their own state (deformation, position) and exteroception to detect information about the external environment (texture, softness, force, slipping, temperature, humidity).

Piezoresistive sensors directly detect deformation based on resistivity with low cost, simple structure, and straightforward detection circuits.[27] Common 3D-printable flexible materials for piezoresistive sensors are CTPU and silicone elastomer

composite with conductive particles. In addition, depending on the functional particles doped in the elastomer, piezoresistive sensors printed via DIW can be used to detect stress, temperature, and humidity changes.[289]

Capacitive sensing feeds back deformation by detecting capacitance changes and has a sensitive response, high bandwidth, and great linearity. Capacitive sensors feature a sandwich structure consisting of conductive electrodes and dielectric elastomers and are commonly used to detect stress. For complex functions, such as slipping detection, a sensor matrix is required to measure the stress changes at different positions.[290] In addition, 3D printing is friendly to constructing complex patterns in electrodes, such as interdigital electrodes, allowing high-DOF design.[291]

Piezoelectric sensors generate an electrical signal to measure material deformation, and their structure is the same as capacitive sensors. The most common 3D-printed piezoelectric material is poly(vinylidene fluoride) (PVDF), a thermoplastic polymer that could be printed via FFF and SC-DW.[288] PVDF film is flexible but nonstretchable, and its strain can be improved via kirigami and auxetics structures.[292]

Multilayer triboelectric sensors detect a charge movement (a current or potential difference) to feedback layer motion when layers with dissimilar materials contact or slip.[293] The triboelectric sensor can be printed integrally with the flexible actuator to detect its bending curvature.[294] Triboelectric sensors are almost exclusively suitable for dynamic measurements and are sensitive to humidity, while this structure is also used for energy harvesting, named triboelectric nanogenerator.[295]

Optical sensors and pneumatic pressure sensors do not generate electrical signals as feedback but rather use light and air pressure changes within a closed chamber to provide feedback on elastic deformation. The optical waveguide provides feedback on tactile sensation and stress by analyzing the energy losses of light through the cavity in the transmission, and the straightforward structure of the optical waveguide can be easily integrated into soft actuators.[296] Pneumatic pressure sensors used for SPA have a simple closed chamber to measure pneumatic pressure based on the ideal gas law.[184] The fabrication of magnetic sensors based on the Hall effect is complex. It involves printing magnetic materials, often using various printing methods to print different components, and then assembling.[297] Printing soft robots with magnetic sensors deserves further research.

Directly printing circuits, sensors, and actuators as a single unit is still a challenge and requires advanced equipment and customized material precursors (filaments, inks, or resins). Most proprioceptive sensors are also influenced by external stimuli. Decoupling allows for more complex information to be processed by combining multiple sensing principles. FFF and DIW-based printing have limited precisions and MJ-based printing is limited in material selection. In some cases, it is necessary to select different printing principles for the various parts of the sensor to fulfill the accuracy and material requirements. Overall, 3D printing is still inferior to traditional processing methods for making ultrathin flexible sensors, such as spin coating. When sensor materials are stiffer than actuator materials, sensors may constrain the deformation amplitude and reduce the range of motion of the soft actuators. In addition, contact sensors put on robotic finger pads may cause motion interference. Sensors with rigid surfaces, like capacitive contact sensors, will diminish the adaptability of the robotic fingers. Designing printable sensors with flexible, stretchable, thin-wall structures is significant for better compatibility.

5. Future Prospects and Conclusions

Iterations in materials science and AM technologies are propelling the development of soft robots. Multimaterial 3D printing technology allows engineers more freedom to design and manufacture functional parts with complex structures. In addition, 3DP enables the fabricating of objects with complex internal structures. We summarized novel soft actuator applications and promising 3DP methods in this section.

5.1. 3D-Printed Physical Intelligence

In traditional mechanics, engineers use threaded connections, gear systems, and rigid printed circuit boards to achieve mechanical connections, drives, and controls, and these traditional methods are limited to soft-bodied robots. Researchers have explored 3D-printed smart materials and structures to encode physical intelligence in soft-bodied robots,[298] enabling intriguing human–robot interactions or compliant robot control systems. For example, logic gates and computation of mechanical systems can be realized by 3D-printed soft convex and concave modules.[299]

Apart from electrical circuits, the digital pneumatic logic gate (PLG) is more suitable for soft robotic systems. One strategy for the PLG is using the hemispherical membrane with snap-through instability.[300,301] The PLG uses a pressure signal to control the adjacent channel pressure on and off. The PLG shows a similar function as the Schmitt trigger and can be used as a soft valve, digital logic gates, set-reset latch, shift register, leading-edge detector, digital-to-analog converter, soft button, toggle switch, and pressure sensor. PLG based on the bistable structure has complex channels and a flexible morphing structure, which is suitable for fabrication by 3D printing (**Figure 11**A).[302] By designing the fluidic channel and trigger structure, the DPL could function like classic electronic metal–oxide–semiconductor field-effect transistors (MOSFETs) with normally open (NO) or normally closed (NC) configurations. The soft robots integrated with soft DLP can work stably after enduring impacts and crush forces. PLG enables gait control of quadruped robots with only one pneumatic channel input, significantly simplifying the design of complex pneumatic systems. In addition to the pneumatic NO/NC transistors, other novel 3D fluidic circuit elements were designed via 3D printing like fluidic diodes (Figure 11B) and fluidic capacitance, etc.[303–305]

The soft body shows high-design DOF in designing functional components. In most cases, controlling pneumatic pressure changes within a tube requires more complex electrical circuits and mechanical structures compared to controlling current changes in an electric wire. At the current stage, the PLG controls the expansion of the cavity through the pure pneumatic circuit to realize the buckle of the adjacent flexible air tube to control the

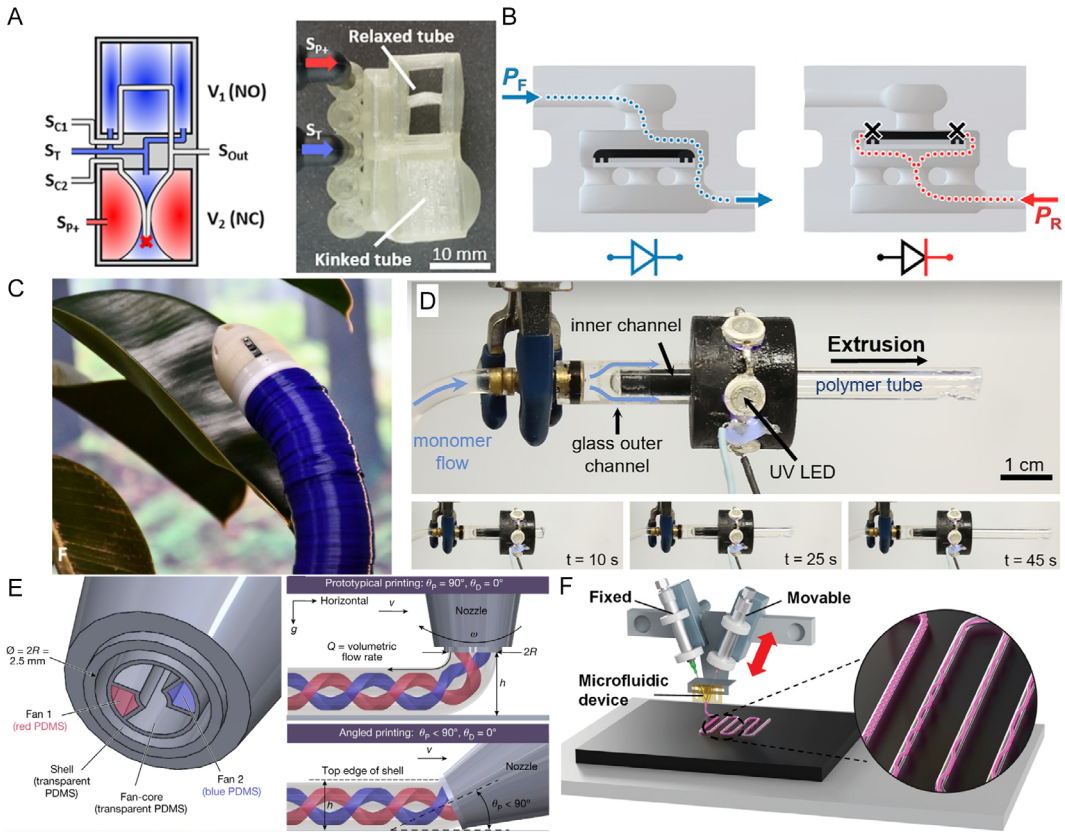

Figure 11. Novel applications and fabrications of 3D-printed soft robots. A,B) 3D-printed pneumatic circuits. (A) FFF-printed TPU valve structure acting as pneumatic NO and NC MOSFET. Reproduced with permission.[302] Copyright 2024, AAAS. (B) PolyJet-printed fluidic diode allowing fluid one-way flow. Reproduced with permission.[303] Copyright 2021, AAAS. C,D) Soft growing robots inspired by AM. (C) FFF-modified growing robot mimicking climbing plants. Reproduced with permission.[309] Copyright 2024, AAAS. (D) VPP-modified growing robot based on self-lubricated photopolymerization extrusion self-navigating in constrained environments and tortuous paths. Reproduced under terms of the CC-BY license.[310] Copyright 2022, The Authors. Published by the United States National Academy of Sciences. E) Subvoxel control based on nozzles with "shell–fan–core" geometry that could program helical angle, layer thickness, and materials of the inner core filaments (red and blue color). Reproduced with permission.[59] Copyright 2023, Springer Nature. F) Subvoxel control based on a microfluidic Y-channel and two printing needles adjusting the position and diameter of inner core filaments. Reproduced under terms of the CC-BY license.[317] Copyright 2024, The Authors. Published by Wiley.

pneumatic circuit on and off. In the future, it may be possible to use multimaterial 3D printing of flexible smart structures to control the on–off of pneumatic circuits through diverse actuation mechanisms (e.g., temperature, humidity, light).

5.2. Growing Robots

Soft growing robots have attracted much attention in recent years for their ability to navigate in unfamiliar environments.[306] Growing robots can mimic plant growth designed by modifying existing 3D printer printheads.[307–309] The FFF-based growth robot consists of a filament feed system at the root and a miniaturized and customized 3D printhead at the tip. In the growing process, the printer nozzle deposited filaments layer by layer to move forward, and the body grew with a tubular shape like a hollow stem (Figure 11C). By adjusting the amount of filament extruded in the circumferential direction, the steering of the growing robot can be adjusted to achieve passage over complex terrain and plant-like climbing behavior. In addition, this growing robot can generate up to 10 N of thrust when encountering obstacles and automatically obstacle avoidance.

Except for fusing thermoplastic filaments, curing photopolymeric resin can be used to design growing robots. Inspired by plants and fungi, Hausladen et al. presented a simple equipment that generates a cured flexible polymer body through a UV LED connecting to a monomer supplying pipe (Figure 11D).[310] The navigation of the polymer body is uncontrollable and passively determined by the environment. The force output of this resin-based growing robot is inferior to the FFF-based one but shows a smaller size and faster-growing speed (almost 12 cm min^{-1}).

Research on soft growing robots derived from 3D printing technology remains limited, as the field is still in its infancy. The 3D-printed growing robot is less affected by pneumatic/hydraulic pressure and can be used in exploration in space and deep sea. The current growing robots are constructed with single materials and simple structures. Future optimizations could involve growing functional structures using composites, multimaterials, or novel growth mechanisms.

5.3. Multimodal Soft Robots

Soft robots have demonstrated excellent performance and even surpassed traditional rigid robots in specific applications. However, in practice, the problems faced by robots are often complex and unstructured.

Soft actuators are widely available for robotic manipulation because of their great adaptability in industrial production. However, for humanoid robots, open environments and complex scenarios demand more from the soft gripper, such as in-hand manipulation or bimanual handling.[311] In addition to vision-based computer aids, multimodal soft grippers combining

Table 2. A summary of 3D-printed soft robotic applications.

Categories	Printing method	Materials	Mechanisms
Grippers	FDM	PLA, TPU, SMP, and their composites	Passive structure,[113,114,313] SPA,[105,107,110,112,117,118,230,243,263,326] cable-driven,[23,104,109] variable stiffness,[26,28] DEA,[236] electroadhesion[238]
	DIW	Silicone elastomer, hydrogel, SMP, and their composites	Variable stiffness,[130] SPA,[134] 4DP hydrogel[234,235]
	VPP	PU-like polymer, hydrogel, LMPC, hydrogel, SMP, and their composites	Vacuum adhesion,[237] LMPC gripper,[233] magnetic gripper,[175] 4DP hydrogel,[165,167] variable stiffness,[163] SPA[156,159,160]
	MJ	Silicone elastomer, SMP	SPA,[176,178–180,183,184] variable stiffness,[185–187,190] dry adhesion,[218] cable driven[251]
	SLS	Nylon, PU-like polymer, and their composites	Variable stiffness,[201] magnetic gripper[204]
Artificial muscles	FDM	TPU, PCL	Pneumatic artificial muscle[101,240]
	DIW	Silicone elastomer, LCE	Pneumatic artificial muscle,[127] LCE muscle[145]
	VPP	PU-like polymer, LCE	Pneumatic artificial muscle,[154] LCE muscle[171]
	MJ	–	–
	SLS	–	–
Biomedical devices	FDM	TPU	Robotic glove,[240,271,272,326] Prosthetic hand[276]
	DIW	Hydrogel, silicone elastomer, SMP, PLA, PCL, and their composites	Artificial heart,[129] SMP stent,[137,138,274,275] facial paralysis treatment[273]
	VPP	Silicone elastomer, and their composites	Artificial heart,[157] magnetic microrobot[281]
	MJ	Hydrogel, silicone elastomer, and their composites	Magnetic robot for drug delivery[280,282]
	SLS	Stainless steel	Cable-driven surgical robot[284]
Locomotion robots	FDM	TPU, SMA, PLA	Multilegged robot,[111,115] inchworm robot,[253] pipe robot,[261–263] swimming robot,[264,266] amphibious robot[268]
	DIW	Silicone elastomer, LCE, hydrogel, and their composites	Multilegged robot,[128] magnetic robot,[141,146,151,234] rolling robot,[144] inchworm robot,[149] swimming robot[150]
	VPP	PU-like polymer, hydrogel, silicone elastomer, and their composites	Inchworm robot,[156,199] magnetic microrobot,[168,173–175] amphibious robot[267]
	MJ	Silicone elastomer, SMA	Multilegged robot,[177,180,251] inchworm robot[179,252,254]
	SLS	–	–
Sensors-integrated robots	FDM	CTPU, CPLA	Piezoresistive strain sensor,[106,112] Piezoresistive pressure sensor,[25,27] Capacitive flex sensor[291]
	DIW	Silicone elastomer, PVDF, ceramic, and their composites	Piezoresistive multiresponsive sensor.[289] Piezoelectric nanogenerator,[292] magnetic inductive force sensor.[297]
	VPP	Silicone elastomer, hydrogel, LCE, and their composites	Piezoresistive temperature sensor.[327–334] Piezoelectric pressure sensor.[327]
	MJ	Silicone elastomer and their composites	Pneumatic pressure sensor,[184] triboelectric curvature sensor[294]
	SLS	Nylon and their composites	Piezoresistive strain sensor.[206,208]
Other applications	FDM	TPU, PLA	PLG,[107,302] growing robot[307–309]
	DIW	Flexible resin	growing robot[310]
	VPP	–	–
	MJ	Silicone elastomer and their composites	Electrical logic gate,[299] PLG[303,304]
	SLS	–	–

different actuation mechanisms can improve grippers' performance, like an octopus that hunts prey with tentacles with suction cups.[312] 3D printing can easily build soft actuators integrated with functional structures like passive fin ray structure,[313] particle jamming,[186] electroadhesion,[238] vacuum suction caps,[237] et al. Multimaterial and cross-scale 3D printing is essential to building soft robots with multiple sections having various functions and paves the road for producing multistimulus or multimodal soft robots. Multistimulus soft robots can easily solve the decoupling problem for robots with multiple tasks, such as a microrobot for drug delivery requiring locomotion and grasping, and multiple stimuli (like ultrasound and magnetic field) can control the two functions independently without any interference.[234]

Another type of multimodal robot can adapt to different environments by changing its actuation strategy. For example, untethered magnetoresponsive locomotion robots can generate up to 12 motion modes (climbing, swimming, walking, rolling, crawling, jumping, etc) based on magnetic field changes when facing different terrains.[314] Variable stiffness structures can change the properties of mechanical parts like natural muscles. In soft amphibious robots, like robotic turtles, the shape and stiffness of flippers are variable for walking on sand or swimming under the sea.[315] Reconfigurable structures allow robots to perform more tasks better without sacrificing other properties.

5.4. Structured Design with Subvoxel Control

Iterations in 3D printing technology have not only allowed engineers to print fine structures more quickly with new materials but have also pushed the limits of some precision machining. To print a single structure with diverse mechanical properties in different regions, voxel control is an effective way, like grayscale DLP.[316]

In the case of DIW, traditional 3D printing is limited to the voxel scale by adjusting the type of ink to achieve multimaterial printing. 3D printing with subvoxel control has become a hot point in recent years. Lewis's team presented a RM-3DP platform that enables subvoxel control over the local orientation of azimuthally heterogeneous architected filaments (Figure 11E).[59] The nozzle of RM-3DP has a "shell–fan–core" geometry, and the fan can rotate in the shell to construct a 3D subvoxel pattern. Helical DEA filaments with programmable helical electrodes and dielectric elastomer matrix were printed via RM-3DP, which displays axial contraction and twisting by applying voltage. The DIW platform can be modified with a movable needle in a Y-shaped microfluidic nozzle to achieve subvoxel control (Figure 11F).[317] This strategy has a simple structure and enables the position control of the inner ink. Fiber filament is the basic structure of natural muscles, and subvoxel control techniques enable artificial muscle design with more complex structures.

The development of 3D/4D-printed soft actuators not only benefits from the progress in materials science and 3D printing mechanisms but also from smart control strategies that enhance the printing precision.[251] Vision-based and AI-assisted 3D printing, incorporating closed-loop correction, offers new possibilities for postprocessing-free SPA fabrication and in situ 3D printing to maintain soft robots.[318–320] The low cost and light weight of 3D-printed soft robots exhibit promising application scenarios in drone manipulation and companion robots and beyond.[321,322]

We have summarized the applications of 3D printed soft robots and the associated printing techniques as shown in **Table 2**. Currently, FFF is the most popular printing method because of its affordability and user-friendly operation. However, FFF is limited to printing thermoplastic polymers. There might be future growth in FFF-based soft robots using functional composites, such as flexible electroadhesion pads by mixing conductive particles into TPU elastomer. Benefiting from material diversity and capability for multiple material printing, DIW shows development prospects, especially in biocompatible material printing and biomedical applications. VPP is essential for producing precision and high-strength parts due to its isotropic product properties and high printing resolution. Future developments in VPP are anticipated to expand compatibility with more materials, increase printing speeds, and support multimaterial printing. The availability of materials and high costs currently restrict the applications of MJ. Printing robust and long-lifetime soft actuators is still a challenge for MJ.

Soft robots have demonstrated irreplaceable capabilities for specific applications. The advancements in 3D printing technology have enabled researchers to explore new actuation principles and iterate on soft robots at an accelerated pace, laying a solid foundation for the future commercialization of soft robots. The future society will be coexisting with soft and rigid robots. The complex interdisciplinary nature of soft robots requires researcher collaboration across various disciplines, such as mechanical engineering, materials science, biology, and computer science, to effectively address the needs of individuals in activities of daily life and industry. We hope that the challenges and innovations discussed in this review on AM, 3D printable materials, soft actuators, and soft robotic applications can break down disciplinary barriers for researchers from diverse fields and provide new inspiration for future research.

Acknowledgements

This work was supported in part by the grants from Research Grants Council of the Hong Kong Special Administrative Region (Theme-based Research scheme no. T42-717/20-R and Strategic Topics grant no. STG1/E-401/23-N).

Conflict of Interest

The authors declare no conflict of interest.

Author Contributions

Hao Liu: conceptualization (equal); data curation (lead); formal analysis (lead); investigation (lead); methodology (lead); software (lead); validation (lead); visualization (lead); writing—original draft (lead). **Changchun Wu**: data curation (equal); formal analysis (equal); investigation (equal); methodology (equal); validation (equal); visualization (equal); writing—original draft (supporting). **Senyuan Lin**: data curation (supporting); formal analysis (supporting); methodology (supporting); validation (supporting); visualization (supporting). **James Lam**: resources (equal); supervision (equal); writing—review & editing (equal). **Ning Xi**: funding acquisition

(lead); project administration (lead); resources (equal); writing—review & editing (supporting). **Yonghua Chen**: conceptualization (lead); funding acquisition (equal); investigation (equal); methodology (equal); project administration (equal); resources (lead); supervision (lead); writing—review & editing (lead).

Keywords

3D printing, additive manufacturing, robotic applications, soft actuators, soft robots

Received: August 14, 2024
Revised: March 3, 2025
Published online: March 14, 2025

[1] D. Rus, M. T. Tolley, *Nature* **2015**, *521*, 467.
[2] N. El-Atab, R. B. Mishra, F. Al-Modaf, L. Joharji, A. A. Alsharif, H. Alamoudi, M. Diaz, N. Qaiser, M. M. Hussain, *Adv. Intell. Syst.* **2020**, *2*, 2000128.
[3] M. Li, A. Pal, A. Aghakhani, A. Pena-Francesch, M. Sitti, *Nat. Rev. Mater.* **2021**, *7*, 235.
[4] E. W. Hawkes, C. Majidi, M. T. Tolley, *Sci. Rob.* **2021**, *6*, eabg6049.
[5] J. D. W. Madden, N. A. Vandesteeg, P. A. Anquetil, P. G. A. Madden, A. Takshi, R. Z. Pytel, S. R. Lafontaine, P. A. Wieringa, I. W. Hunter, *IEEE J. Oceanic Eng.* **2004**, *29*, 706.
[6] S. Coyle, C. Majidi, P. LeDuc, K. J. Hsia, *Extreme Mech. Lett.* **2018**, *22*, 51.
[7] R. F. Shepherd, F. Ilievski, W. Choi, S. A. Morin, A. A. Stokes, A. D. Mazzeo, X. Chen, M. Wang, G. M. Whitesides, *Proc. Natl. Acad. Sci. U.S.A.* **2011**, *108*, 20400.
[8] K. Bertoldi, V. Vitelli, J. Christensen, M. van Hecke, *Nat. Rev. Mater.* **2017**, *2*, 1.
[9] I. Apsite, S. Salehi, L. Ionov, *Chem. Rev.* **2021**, *122*, 1349.
[10] B. Jumet, M. D. Bell, V. Sanchez, D. J. Preston, *Adv. Intell. Syst.* **2022**, *4*, 2100163.
[11] L. Zhou, J. Fu, Y. He, *Adv. Funct. Mater.* **2020**, *30*, 2000187.
[12] L. Tang, J. Shang, X. Jiang, *Sci. Adv.* **2021**, *7*, eabe3778.
[13] B. Gorissen, T. Chishiro, S. Shimomura, D. Reynaerts, M. De Volder, S. Konishi, *Sens. Actuators, A* **2014**, *216*, 426.
[14] D. Duanmu, X. Wang, X. Li, Z. Wang, Y. Hu, *Actuators* **2022**, *11*, 346.
[15] N. Shahrubudin, T. C. Lee, R. Ramlan, *Procedia Manuf.* **2019**, *35*, 1286.
[16] H. K. Yap, P. M. Khin, T. H. Koh, Y. Sun, X. Liang, J. H. Lim, C.-H. Yeow, *IEEE Rob. Autom. Lett.* **2017**, *2*, 1383.
[17] M. Feng, D. Yang, L. Ren, G. Wei, G. Gu, *Sci. Adv.* **2023**, *9*, eadi7133.
[18] H. D. Yang, A. T. Asbeck, *Soft Rob.* **2020**, *7*, 218.
[19] X. Meng, S. Li, X. Shen, C. Tian, L. Mao, H. Xie, *Nat. Commun.* **2024**, *15*, 10442.
[20] D. Drummer, S. Cifuentes-Cuéllar, D. Rietzel, *Rapid Prototyping J.* **2012**, *18*, 500.
[21] E. Soleyman, M. Aberoumand, D. Rahmatabadi, K. Soltanmohammadi, I. Ghasemi, M. Baniassadi, K. Abrinia, M. Baghani, *J. Mater. Res. Technol.* **2022**, *18*, 4201.
[22] S. Wojtyła, P. Klama, T. Baran, *J. Occup. Environ. Hyg.* **2017**, *14*, D80.
[23] C. Tawk, A. Gillett, M. in het Panhuis, G. M. Spinks, G. Alici, *IEEE Trans. Rob.* **2019**, *35*, 1268.
[24] M. León-Calero, S. C. Reyburn Valés, Á. Marcos-Fernández, J. Rodríguez-Hernandez, *Polymers* **2021**, *13*, 3551.
[25] M. Alsharari, B. Chen, W. Shu, *Adv. Electron. Mater.* **2021**, *8*, 2100597.
[26] Y. Yang, Y. Chen, Y. Wei, Y. Li, *Int. J. Adv. Manuf. Technol.* **2016**, *84*, 2079.
[27] Y. Yang, Y. Chen, Y. Li, Z. Wang, Y. Li, *Soft Rob.* **2017**, *4*, 338.
[28] M. Al-Rubaiai, T. Pinto, C. Qian, X. Tan, *Soft Rob.* **2019**, *6*, 318.
[29] G. Chatzipirpiridis, S. Gervasoni, C. Fischer, O. Ergeneman, E. Pellicer, B. J. Nelson, S. Pané, *Adv. Intell. Syst.* **2019**, *1*, 1900069.
[30] H. Ye, Q. Liu, J. Cheng, H. Li, B. Jian, R. Wang, Z. Sun, Y. Lu, Q. Ge, *Nat. Commun.* **2023**, *14*, 1607.
[31] M. A. Saadi, A. Maguire, N. T. Pottackal, M. S. Thakur, M. Md. Ikram, A. J. Hart, P. M. Ajayan, M. M. Rahman, *Adv. Mater.* **2022**, *34*, 2108855.
[32] M. Champeau, D. A. Heinze, T. N. Viana, E. R. de Souza, A. C. Chinellato, S. Titotto, *Adv. Funct. Mater.* **2020**, *30*, 1910606.
[33] D. A. Porter, A. L. Cohen, P. S. Krueger, D. Y. Son, *3D Print. Addit. Manuf.* **2018**, *5*, 73.
[34] L. Li, Q. Lin, M. Tang, A. J. Duncan, C. Ke, *Chem. Eur. J.* **2019**, *25*, 10768.
[35] C. F. Revelo, H. A. Colorado, *Ceram. Int.* **2018**, *44*, 5673.
[36] B. Y. Ahn, D. Shoji, C. J. Hansen, E. Hong, D. C. Dunand, J. A. Lewis, *Adv. Mater.* **2010**, *22*, 2251.
[37] H. Dong, T. Weng, K. Zheng, H. Sun, B. Chen, *3D Print. Addit. Manuf.* **2024**, *11*, 954.
[38] Y. Xia, Z. Lu, J. Cao, K. Miao, J. Li, D. Li, *Scr. Mater.* **2019**, *165*, 84.
[39] H. W. Kang, S. J. Lee, I. K. Ko, C. Kengla, J. J. Yoo, A. Atala, *Nat. Biotechnol.* **2016**, *34*, 312.
[40] D. Periard, N. Schaal, M. Schaal, E. Malone, H. Lipson, in *2007 Int. Solid Freeform Fabrication Symp.*, The University of Texas at Austin, Austin, TX, August **2007**, pp. 564–574.
[41] S. Guo, F. Gosselin, N. Guerin, A. M. Lanouette, M. C. Heuzey, D. Therriault, *Small* **2013**, *9*, 4118.
[42] G. Postiglione, G. Natale, G. Griffini, M. Levi, S. Turri, *Composites, Part A* **2015**, *76*, 110.
[43] A. D. Valino, J. R. C. Dizon, A. H. Espera Jr, Q. Chen, J. Messman, R. C. Advincula, *Prog. Polym. Sci.* **2019**, *98*, 101162.
[44] S. Chandrasekaran, E. B. Duoss, M. A. Worsley, J. P. Lewicki, *J. Mater. Chem. A* **2018**, *6*, 853.
[45] Q. Chen, P. F. Cao, R. C. Advincula, *Adv. Funct. Mater.* **2018**, *28*, 1800631.
[46] S. Roh, D. P. Parekh, B. Bharti, S. D. Stoyanov, O. D. Velev, *Adv. Mater.* **2017**, *29*, 1701554.
[47] L. Y. Zhou, Q. Gao, J. Z. Fu, Q. Y. Chen, J. P. Zhu, Y. Sun, Y. He, *ACS Appl. Mater. Interfaces* **2019**, *11*, 23573.
[48] D. M. Kirchmajer, R. Gorkin Iii, *J. Mater. Chem. B* **2015**, *3*, 4105.
[49] Z. Lyu, J. J. Koh, G. J. Lim, D. Zhang, T. Xiong, L. Zhang, S. Liu, J. Duan, J. Ding, J. Wang, J. Wang, Y. Chen, C. He, *Interdiscip. Mater.* **2022**, *1*, 507.
[50] O. D. Yirmibesoglu, L. E. Simonsen, R. Manson, J. Davidson, K. Healy, Y. Menguc, T. Wallin, *Commun. Mater.* **2021**, *2*, 82.
[51] W. Liu, Y. S. Zhang, M. A. Heinrich, F. De Ferrari, H. L. Jang, S. M. Bakht, M. M. Alvarez, J. Yang, Y. Li, G. Trujillo-de Santiago, A. K. Miri, K. Zhu, P. Khoshakhlagh, G. Prakash, H. Cheng, X. Guan, Z. Zhong, J. Ju, G. H. Zhu, X. Jin, S. R. Shin, M. R. Dokmeci, A. Khademhosseini, *Adv. Mater.* **2016**, *29*, 1604630.
[52] J. O. Hardin, T. J. Ober, A. D. Valentine, J. A. Lewis, *Adv. Mater.* **2015**, *27*, 3279.
[53] J. Yin, M. Li, G. Dai, H. Zhou, L. Ma, Y. Zheng, *J. Bionic Eng.* **2021**, *18*, 346.
[54] O. Byrne, F. Coulter, M. Glynn, J. F. Jones, A. Ní Annaidh, E. D. O'Cearbhaill, D. P. Holland, *Soft Rob.* **2018**, *5*, 726.
[55] T. J. Ober, D. Foresti, J. A. Lewis, *Proc. Natl. Acad. Sci. U.S.A.* **2015**, *112*, 12293.
[56] D. J. Lorang, D. Tanaka, C. M. Spadaccini, K. A. Rose, N. J. Cherepy, J. A. Lewis, *Adv. Mater.* **2011**, *23*, 5055.
[57] J. Mueller, J. R. Raney, K. Shea, J. A. Lewis, *Adv. Mater.* **2018**, *30*, 1705001.

[58] M. A. Skylar-Scott, J. Mueller, C. W. Visser, J. A. Lewis, *Nature* **2019**, *575*, 330.
[59] N. M. Larson, J. Mueller, A. Chortos, Z. S. Davidson, D. R. Clarke, J. A. Lewis, *Nature* **2023**, *613*, 682.
[60] V. S. Joseph, T. Calais, T. Stalin, S. Jain, N. K. Thanigaivel, N. D. Sanandiya, P. Valdivia y Alvarado, *Appl. Mater. Today* **2021**, *22*, 100979.
[61] G. Shi, S. E. Lowe, A. J. T. Teo, T. K. Dinh, S. H. Tan, J. Qin, Y. Zhang, Y. L. Zhong, H. Zhao, *Appl. Mater. Today* **2019**, *16*, 482.
[62] X. Wan, L. Luo, Y. Liu, J. Leng, *Adv. Sci.* **2020**, *7*, 2001000.
[63] V. G. Rocha, E. Saiz, I. S. Tirichenko, E. García-Tuñón, *J. Mater. Chem. A* **2020**, *8*, 15646.
[64] H. Wang, B. Zhang, J. Zhang, X. He, F. Liu, J. Cui, Z. Lu, G. Hu, J. Yang, Z. Zhou, R. Wang, X. Hou, L. Ma, P. Ren, Q. Ge, P. Li, W. Huang, *ACS Appl. Mater. Interfaces* **2021**, *13*, 55507.
[65] S. Walker, U. Daalkhaijav, D. Thrush, C. Branyan, O. D. Yirmibesoglu, G. Olson, Y. Menguc, *3D Print. Addit. Manuf.* **2019**, *6*, 139.
[66] J. Wang, S. Yang, P. Ding, X. Cao, Y. Zhang, S. Cao, K. Zhang, S. Kong, Y. Zhou, X. Wang, D. Li, D. Kong, *ACS Appl. Mater. Interfaces* **2019**, *11*, 18590.
[67] M. Shusteff, A. E. Browar, B. E. Kelly, J. Henriksson, T. H. Weisgraber, R. M. Panas, N. X. Fang, C. M. Spadaccini, *Sci. Adv.* **2017**, *3*, eaao5496.
[68] M. Pagac, J. Hajnys, Q.-P. Ma, L. Jancar, J. Jansa, P. Stefek, J. Mesicek, *Polymers* **2021**, *13*, 598.
[69] W. Zhao, Z. Wang, J. Zhang, X. Wang, Y. Xu, N. Ding, Z. Peng, *Adv. Mater. Technol.* **2021**, *6*, 2001218.
[70] C. Decker, T. N. T. Viet, D. Decker, E. Weber-Koehl, *Polymer* **2001**, *42*, 5531.
[71] A. Al Rashid, W. Ahmed, M. Y. Khalid, M. Koc, *Addit. Manuf.* **2021**, *47*, 102279.
[72] A. Andreu, P.-C. Su, J.-H. Kim, C. S. Ng, S. Kim, I. Kim, J. Lee, J. Noh, A. S. Subramanian, Y.-J. Yoon, *Addit. Manuf.* **2021**, *44*, 102024.
[73] R. Wicker, F. Medina, C. Elkins, in *2004 Int. Solid Freeform Fabrication Symp.*, The University of Texas at Austin, Austin, TX, August **2004**, pp. 754–764.
[74] D. K. Patel, A. H. Sakhaei, M. Layani, B. Zhang, Q. Ge, S. Magdassi, *Adv. Mater.* **2017**, *29*, 1606000.
[75] J. M. Sirrine, A. Zlatanic, V. Meenakshisundaram, J. M. Messman, C. B. Williams, P. R. Dvornic, T. E. Long, *Macromol. Chem. Phys.* **2019**, *220*, 1800425.
[76] H. Liu, R. Liu, K. Chen, Y. Liu, Y. Zhao, X. Cui, Y. Tian, *J. Chem. Eng.* **2023**, *461*, 141966.
[77] M. Yin, M. Yao, S. Gao, A. Zhang, H. Tam, P. Wai, *Adv. Mater.* **2015**, *28*, 1394.
[78] L. J. Tan, W. Zhu, K. Zhou, *Adv. Funct. Mater.* **2020**, *30*, 2003062.
[79] Y. Yagci, S. Jockusch, N. J. Turro, *Macromolecules* **2010**, *43*, 6245.
[80] S. Lantean, G. Barrera, C. F. Pirri, P. Tiberto, M. Sangermano, I. Roppolo, G. Rizza, *Adv. Mater. Technol.* **2019**, *4*, 1900505.
[81] F. Zhang, L. Zhu, Z. Li, S. Wang, J. Shi, W. Tang, N. Li, J. Yang, *Addit. Manuf.* **2021**, *48*, 102423.
[82] P. J. Bártolo, *Stereolithography: Materials, Processes and Applications*, Springer Science & Business Media, Berlin, Germany **2011**.
[83] J. W. Choi, H. C. Kim, R. Wicker, *J. Mater. Process. Technol.* **2011**, *211*, 318.
[84] C. D. Matte, M. Pearson, F. Trottier-Cournoyer, A. Dafoe, T. H. Kwok, *Rapid Prototyping J.* **2019**, *25*, 864.
[85] L. H. Han, S. Suri, C. E. Schmidt, S. Chen, *Biomed. Microdevices* **2010**, *12*, 721.
[86] K. Kowsari, S. Akbari, D. Wang, N. X. Fang, Q. Ge, *3D Print. Addit. Manuf.* **2018**, *5*, 185.
[87] D. Han, C. Yang, N. X. Fang, H. Lee, *Addit. Manuf.* **2019**, *27*, 606.
[88] J. J. Schwartz, A. J. Boydston, *Nat. Commun.* **2019**, *10*, 791.
[89] H. Mao, W. Jia, Y. S. Leung, J. Jin, Y. Chen, *Rapid Prototyp. J.* **2021**, *27*, 861.
[90] P. Pandey, M. Taufik, in *Recent Advances in Mechanical Engineering: Select Proc. of CAMSE 2021*, Springer, Singapore, September **2022**, pp. 401–410.
[91] O. Gülcan, K. Günaydın, A. Tamer, *Polymers* **2021**, *13*, 2829.
[92] A. Elkaseer, K. J. Chen, J. C. Janhsen, O. Refle, V. Hagenmeyer, S. G. Scholz, *Addit. Manuf.* **2022**, *60*, 103270.
[93] D. McCoul, S. Rosset, S. Schlatter, H. Shea, *Smart Mater. Struct.* **2017**, *26*, 125022.
[94] C. Sturgess, C. J. Tuck, I. A. Ashcroft, R. D. Wildman, *J. Mater. Chem. C* **2017**, *5*, 9733.
[95] M. Mehrpouya, D. Tuma, T. Vaneker, M. Afrasiabi, M. Bambach, I. Gibson, *Rapid Prototyping J.* **2022**, *28*, 1.
[96] V. V. Popov, M. L. Grilli, A. Koptyug, L. Jaworska, A. Katz-Demyanetz, D. Klobčar, S. Balos, B. O. Postolnyi, S. Goel, *Materials* **2021**, *14*, 909.
[97] S. K. Tiwari, S. Pande, S. Agrawal, S. M. Bobade, *Rapid Prototyping J.* **2015**, *21*, 630.
[98] J. Whitehead, H. Lipson, *Addit. Manuf.* **2020**, *36*, 101440.
[99] I. Gibson, D. Rosen, B. Stucker, M. Khorasani, *Additive Manufacturing Technologies*, Springer, Cham, Switzerland, **2021**.
[100] N. Jayanth, P. Senthil, C. Prakash, *Virtual Phys. Prototyping* **2018**, *13*, 155.
[101] K. Han, N. H. Kim, D. Shin, *Soft Rob.* **2018**, *5*, 554.
[102] A. Altelbani, H. Zhou, S. Mehrdad, F. Alambeigi, S. F. Atashzar, *IEEE Rob. Autom. Lett.* **2021**, *6*, 7941.
[103] M. Smith, V. Cacucciolo, H. Shea, *Science* **2023**, *379*, 1327.
[104] H. Liu, C. Wu, S. Lin, Y. Li, Y. Chen, *Biomimetics* **2022**, *7*, 171.
[105] W. Kim, J. Eom, K. J. Cho, *Adv. Intell. Syst.* **2022**, *4*, 2100176.
[106] T. Hainsworth, L. Smith, S. Alexander, R. MacCurdy, *IEEE Rob. Autom. Lett.* **2020**, *5*, 4118.
[107] Y. Zhai, A. De Boer, J. Yan, B. Shih, M. Faber, J. Speros, R. Gupta, M. T. Tolley, *Sci. Rob.* **2023**, *8*, eadg3792.
[108] Y. Wu, Z. Dai, H. Liu, L. Wang, M. P. Nemitz, in *2024 IEEE Int. Conf. on Soft Robotics (RoboSoft)*, IEEE, San Diego, CA, May **2024**, pp. 249–254.
[109] C. Tawk, G. M. Spinks, M. in het Panhuis, G. Alici, *IEEE/ASME Trans. Mechatron.* **2019**, *24*, 2118.
[110] Y. Yang, Y. Li, Y. Chen, Y. Li, T. Ren, Y. Ren, *IEEE Access* **2020**, *8*, 155912.
[111] Y. Yang, S. Yan, M. Dai, Y. Xie, J. Liu, in *Chinese Intelligent Automation Conf.*, Springer Nature Singapore, Singapore, Nanjing, China, September **2023**, pp. 417–426.
[112] Y. Yang, S. Yan, Y. Xie, Y. Wang, J. Liu, Y. Li, J. Zhou, *IEEE Rob. Autom. Lett.* **2023**, *9*, 1404.
[113] W. Crooks, G. Vukasin, M. O'Sullivan, W. Messner, C. Rogers, *Front. Rob. AI.* **2016**, *3*, 70.
[114] J. H. Shin, J. G. Park, D. I. Kim, H. S. Yoon, *Int. J. Precis. Eng. Manuf. - Green Technol.* **2021**, *8*, 889.
[115] P. Manoonpong, H. Rajabi, J. C. Larsen, S. S. Raoufi, N. Asawalertsak, J. Homchanthanakul, H. T. Tramsen, A. Darvizeh, S. N. Gorb, *Adv. Intell. Syst.* **2022**, *4*, 2100133.
[116] W. Shan, T. Lu, C. Majidi, *Smart Mater. Struct.* **2013**, *22*, 085005.
[117] Y. Yang, Y. Chen, Y. Li, M. Z. Chen, Y. Wei, *Soft Rob.* **2017**, *4*, 147.
[118] Y. Yang, H. Zhu, J. Liu, Z. Wei, Y. Li, J. Zhou, *IEEE Trans. Instrum. Meas.* **2023**, *72*, 1.
[119] D. Ke, Z. Chen, Z. Y. Momo, W. Jiani, C. Xuan, Y. Xiaojie, X. Xueliang, *Smart Mater. Struct.* **2020**, *29*, 023001.
[120] Y. Zhou, Y. Yang, A. Jian, T. Zhou, G. Tao, L. Ren, J. Zang, Z. Zhang, *Compos. Technol.* **2022**, *227*, 109603.
[121] Y. Wang, H. Ye, J. He, Q. Ge, Y. Xiong, *Nat. Commun.* **2024**, *15*, 2322.

[122] M. Y. Khalid, Z. U. Arif, W. Ahmed, *Macromol. Mater. Eng.* **2022**, *307*, 2200003.
[123] W. Zhao, F. Zhang, J. Leng, Y. Liu, *Compos. Technol.* **2019**, *184*, 107866.
[124] M. Aberoumand, D. Rahmatabadi, A. Aminzadeh, M. Moradi, *Fused Deposition Modeling Based 3D Printing*, Springer Nature Singapore, Singapore **2021**.
[125] S. Chen, J. Hu, H. Zhuo, *Compos. Technol.* **2010**, *70*, 1437.
[126] L. Cecchini, S. Mariani, M. Ronzan, A. Mondini, N. M. Pugno, B. Mazzolai, *Adv. Sci.* **2023**, *10*, 2205146.
[127] M. Schaffner, J. A. Faber, L. Pianegonda, P. A. Rühs, F. Coulter, A. R. Studart, *Nat. Commun.* **2018**, *9*, 878.
[128] O. D. Yirmibesoglu, J. Morrow, S. Walker, W. Gosrich, R. Cañizares, H. Kim, U. Daalkhaijav, C. Fleming, C. Branyan, Y. Menguc, in *2018 IEEE Int. Conf. Soft Robotics (RoboSoft)*, IEEE, Livorno, Italy, July **2018**, pp. 295–302.
[129] Y. Cheng, K. H. Chan, X.-Q. Wang, T. Ding, T. Li, X. Lu, G. W. Ho, *ACS Nano* **2019**, *13*, 13176.
[130] B. J. Cafferty, V. E. Campbell, P. Rothemund, D. J. Preston, A. Ainla, N. Fulleringer, A. C. Diaz, A. E. Fuentes, D. Sameoto, J. A. Lewis, G. M. Whitesides, *Adv. Mater. Technol.* **2018**, *4*, 1800299.
[131] W. Wu, A. DeConinck, J. A. Lewis, *Adv. Mater.* **2011**, *23*, H178.
[132] R. D. Weeks, R. L. Truby, S. G. Uzel, J. A. Lewis, *Adv. Mater.* **2023**, *35*, 2206958.
[133] M. Wehner, R. L. Truby, D. J. Fitzgerald, B. Mosadegh, G. M. Whitesides, J. A. Lewis, R. J. Wood, *Nature* **2016**, *536*, 451.
[134] Y. Li, Z. Wu, Y. Chen, S. Xian, Z. Hong, Q. Wang, P. Jiang, H. Yu, Y. Zhong, *Addit. Manuf.* **2024**, *85*, 104178.
[135] R. Su, J. Wen, Q. Su, M. S. Wiederoder, S. J. Koester, J. R. Uzarski, M. C. McAlpine, *Sci. Adv.* **2020**, *6*, eabc9846.
[136] G. H. Koo, J. Jang, *J. Appl. Polym.* **2013**, *127*, 4515.
[137] H. Wei, Q. Zhang, Y. Yao, L. Liu, Y. Liu, J. Leng, *ACS Appl. Mater. Interfaces* **2017**, *9*, 876.
[138] X. Wan, H. Wei, F. Zhang, Y. Liu, J. Leng, *J. Appl. Polym.* **2019**, *136*, 48177.
[139] X. Wan, F. Zhang, Y. Liu, J. Leng, *Carbon* **2019**, *155*, 77.
[140] A. S. Wu, W. Small IV, T. M. Bryson, E. Cheng, T. R. Metz, S. E. Schulze, E. B. Duoss, T. S. Wilson, *Sci. Rep.* **2017**, *7*, 4664.
[141] Y. Kim, H. Yuk, R. Zhao, S. A. Chester, X. Zhao, *Nature* **2018**, *558*, 274.
[142] Y. Zhang, X. Y. Yin, M. Zheng, C. Moorlag, J. Yang, Z. L. Wang, *J. Mater. Chem. A* **2019**, *7*, 6972.
[143] J. Zhao, L. Zhang, J. Hu, *Adv. Intell. Syst.* **2022**, *4*, 2100065.
[144] A. Kotikian, C. McMahan, E. C. Davidson, J. M. Muhammad, R. D. Weeks, C. Daraio, J. A. Lewis, *Sci. Rob.* **2019**, *4*, eaax7044.
[145] J. Liu, Y. Gao, H. Wang, R. Poling-Skutvik, C. O. Osuji, S. Yang, *Adv. Intell. Syst.* **2020**, *2*, 1900163.
[146] Y. Sun, L. Wang, Z. Zhu, X. Li, H. Sun, Y. Zhao, C. Peng, J. Liu, S. Zhang, M. Li, *Adv. Mater.* **2023**, *35*, 2302824.
[147] K. Kim, Y. Guo, J. Bae, S. Choi, H. Y. Song, S. Park, K. Hyun, S. Ahn, *Small* **2021**, *17*, 2100910.
[148] C. Yang, Z. Suo, *Nat. Rev. Mater.* **2018**, *3*, 125.
[149] A. Pantula, B. Datta, Y. Shi, M. Wang, J. Liu, S. Deng, N. J. Cowan, T. D. Nguyen, D. H. Gracias, *Sci. Rob.* **2022**, *7*, eadd2903.
[150] H. Zhu, B. Xu, Y. Wang, X. Pan, Z. Qu, Y. Mei, *Sci. Rob.* **2021**, *6*, eabe7925.
[151] B. Sun, R. Jia, H. Yang, X. Chen, K. Tan, Q. Deng, J. Tang, *Adv. Intell. Syst.* **2022**, *4*, 2100139.
[152] Y. Luo, X. Lin, B. Chen, X. Wei, *Biofabrication* **2019**, *11*, 045019.
[153] S. Khetan, L. H. Blumenschein, *IEEE Rob. Autom. Lett.* **2022**, *7*, 5342.
[154] C. De Pascali, G. A. Naselli, S. Palagi, R. B. Scharff, B. Mazzolai, *Sci. Rob.* **2022**, *7*, eabn4155.
[155] G. A. Naselli, R. B. Scharff, M. Thielen, F. Visentin, T. Speck, B. Mazzolai, *Adv. Intell. Syst.* **2025**, *6*, 2300537.
[156] J. Wan, L. Sun, T. Du, *IEEE Access* **2023**, *11*, 86227.
[157] T. J. Wallin, L. E. Simonsen, W. Pan, K. Wang, E. Giannelis, R. F. Shepherd, Y. Mengüç, *Nat. Commun.* **2020**, *11*, 4000.
[158] T. J. Wallin, J. H. Pikul, S. Bodkhe, B. N. Peele, B. C. Mac Murray, D. Therriault, B. W. McEnerney, R. P. Dillon, E. P. Giannelis, R. F. Shepherd, *J. Mater. Chem. B* **2017**, *5*, 6249.
[159] H. Yuk, S. Lin, C. Ma, M. Takaffoli, N. X. Fang, X. Zhao, *Nat. Commun.* **2017**, *8*, 14230.
[160] A. K. Mishra, T. J. Wallin, W. Pan, A. Xu, K. Wang, E. P. Giannelis, B. Mazzolai, R. F. Shepherd, *Sci. Rob.* **2020**, *5*, eaaz3918.
[161] Y. Y. C. Choong, S. Maleksaeedi, H. Eng, J. Wei, P. C. Su, *Mater. Des.* **2017**, *126*, 219.
[162] M. N. I. Shiblee, K. Ahmed, A. Khosla, M. Kawakami, H. Furukawa, *Soft Matter* **2018**, *14*, 7809.
[163] Q. Ge, A. H. Sakhaei, H. Lee, C. K. Dunn, N. X. Fang, M. L. Dunn, *Sci. Rep.* **2016**, *6*, 31110.
[164] B. Peng, Y. Yang, K. Gu, E. J. Amis, K. A. Cavicchi, *ACS Mater. Lett.* **2019**, *1*, 410.
[165] D. Han, Z. Lu, S. A. Chester, H. Lee, *Sci. Rep.* **2018**, *8*, 1963.
[166] Z. Zhao, X. Kuang, C. Yuan, H. J. Qi, D. Fang, *ACS Appl. Mater. Interfaces* **2018**, *10*, 19932.
[167] D. Han, C. Farino, C. Yang, T. Scott, D. Browe, W. Choi, J. W. Freeman, H. Lee, *ACS Appl. Mater. Interfaces* **2018**, *10*, 17512.
[168] X. Wang, X. Qin, C. Hu, A. Terzopoulou, X. Chen, T. Huang, K. Maniura-Weber, S. Pané, B. J. Nelson, *Adv. Funct. Mater.* **2018**, *28*, 1804107.
[169] C. Zheng, F. Jin, Y. Zhao, M. Zheng, J. Liu, X. Dong, Z. Xiong, Y. Xia, X. Duan, *Sens. Actuators, B* **2020**, *304*, 127345.
[170] Z. Wang, Y. Guo, S. Cai, J. Yang, *ACS Appl. Polym. Mater.* **2022**, *4*, 3153.
[171] S. Li, H. Bai, Z. Liu, X. Zhang, C. Huang, L. W. Wiesner, M. Silberstein, R. F. Shepherd, *Sci. Adv.* **2021**, *7*, eabg3677.
[172] L. Chen, Y. Dong, C.-Y. Tang, L. Zhong, W.-C. Law, G. C. Tsui, Y. Yang, X. Xie, *ACS Appl. Mater. Interfaces* **2019**, *11*, 19541.
[173] Z. Li, Y. P. Lai, E. Diller, *Adv. Intell. Syst.* **2024**, *6*, 2300052.
[174] L. Lu, P. Guo, Y. Pan, *J. Manuf. Sci. Eng.* **2017**, *139*, 071008.
[175] E. B. Joyee, A. Szmelter, D. Eddington, Y. Pan, *Soft Rob.* **2022**, *9*, 1.
[176] H. Zhang, A. S. Kumar, J. Y. H. Fuh, M. Y. Wang, *Soft Rob.* **2018**, *5*, 650.
[177] R. MacCurdy, R. Katzschmann, Y. Kim, D. Rus, in *2016 IEEE Int. Conf. Robotics and Automation (ICRA)*, IEEE, Stockholm, Sweden, June **2016**, pp. 3878–3885.
[178] Z. Wang, S. Hirai, *IEEE Rob. Autom. Lett.* **2017**, *2*, 624.
[179] C. Du Pasquier, T. Chen, S. Tibbits, K. Shea, *Soft Rob.* **2019**, *6*, 657.
[180] D. Drotman, M. Ishida, S. Jadhav, M. T. Tolley, *IEEE/ASME Trans. Mechatron.* **2018**, *24*, 78.
[181] J. A. E. Hughes, P. Maiolino, F. Iida, *Sci. Rob.* **2018**, *3*, eaau3098.
[182] M. C. Saldívar, E. Tay, A. Isaakidou, V. Moosabeiki, L. E. Fratila-Apachitei, E. L. Doubrovski, M. J. Mirzaali, A. A. Zadpoor, *Nat. Commun.* **2023**, *14*, 7919.
[183] K. Kumar, J. Liu, C. Christianson, M. Ali, M. T. Tolley, J. Aizenberg, D. E. Ingber, J. C. Weaver, K. Bertoldi, *Soft Rob.* **2017**, *4*, 317.
[184] O. Shorthose, A. Albini, L. He, P. Maiolino, *IEEE Rob. Autom. Lett.* **2022**, *7*, 3945.
[185] M. Zhu, Y. Mori, T. Wakayama, A. Wada, S. Kawamura, *Soft Rob.* **2019**, *6*, 507.
[186] G. D. Howard, J. Brett, J. O'Connor, J. Letchford, G. W. Delaney, *Soft Rob.* **2022**, *9*, 497.
[187] M. Zhu, M. Xie, Y. Mori, J. Dai, S. Kawamura, X. Yue, *Soft Rob.* **2024**, *11*, 85.

[188] S. Schlatter, G. Grasso, S. Rosset, H. Shea, *Adv. Intell. Syst.* **2020**, *2*, 2000136.
[189] B. Hayes, T. Hainsworth, R. MacCurdy, *Addit. Manuf.* **2022**, *55*, 102785.
[190] J. Wu, C. Yuan, Z. Ding, M. Isakov, Y. Mao, T. Wang, M. L. Dunn, H. J. Qi, *Sci. Rep.* **2016**, *6*, 24224.
[191] Z. Ding, O. Weeger, H. J. Qi, M. L. Dunn, *Mater. Des.* **2018**, *137*, 256.
[192] Y. Mao, K. Yu, M. S. Isakov, J. Wu, M. L. Dunn, H. Jerry Qi, *Sci. Rep.* **2015**, *5*, 13616.
[193] C. L. Van Oosten, C. W. Bastiaansen, D. J. Broer, *Nat. Mater.* **2009**, *8*, 677.
[194] S. Yoon, J. A. Park, H. R. Lee, W. H. Yoon, D. S. Hwang, S. Jung, *Adv. Healthcare Mater.* **2018**, *7*, 1800050.
[195] A. Negro, T. Cherbuin, M. P. Lutolf, *Sci. Rep.* **2018**, *8*, 17099.
[196] K. Pataky, T. Braschler, A. Negro, P. Renaud, M. P. Lutolf, J. Brugger, *Adv. Mater.* **2012**, *24*, 391.
[197] Y. Dong, S. Wang, Y. Ke, L. Ding, X. Zeng, S. Magdassi, Y. Long, *Adv. Mater. Technol.* **2020**, *5*, 2000034.
[198] R. B. Scharff, E. L. Doubrovski, W. A. Poelman, P. P. Jonker, C. C. Wang, J. M. Geraedts, in *Soft Robotics: Trends, Applications and Challenges: Proc. of the Soft Robotics Week*, Springer International Publishing, Livorno, Italy, April **2016**, pp. 23–29.
[199] T. Du, L. Sun, J. Wan, *Biomimetics* **2022**, *7*, 205.
[200] J. Guo, J. H. Low, J. Liu, Y. Li, Z. Liu, C. H. Yeow, *Polymers* **2022**, *14*, 3542.
[201] W. Gao, J. Kang, G. Wang, H. Ma, X. Chen, M. Kadic, V. Laude, H. Tan, Y. Wang, *Adv. Intell. Syst.* **2023**, *5*, 2300285.
[202] S. Mei, J. Wang, Z. Li, B. Ding, S. Li, X. Chen, W. Zhao, Y. Zhang, X. Zhang, Z. Cui, P. Fu, X. Pang, M. Liu, *J. Manuf. Processes* **2023**, *92*, 157.
[203] S. Li, Z. Li, S. Mei, X. Chen, B. Ding, Y. Zhang, W. Zhao, X. Zhang, Z. Cui, P. Fu, X. Pang, M. Liu, *Adv. Mater. Technol.* **2023**, *8*, 2202066.
[204] H. Wu, O. Wang, Y. Tian, M. Wang, B. Su, C. Yan, K. Zhou, Y. Shi, *ACS Appl. Mater. Interfaces.* **2020**, *13*, 12679.
[205] H. Ouyang, X. Li, X. Lu, H. Xia, *ACS Appl. Polym. Mater.* **2022**, *4*, 4035.
[206] S. Wei, L. Zhang, C. Li, S. Tao, B. Ding, H. Zhu, S. Xia, *J. Mater. Chem. C* **2019**, *7*, 6786.
[207] A. Ronca, G. Rollo, P. Cerruti, G. Fei, X. Gan, G. G. Buonocore, M. Lavorgna, H. Xia, C. Silvestre, L. Ambrosio, *Appl. Sci.* **2019**, *9*, 864.
[208] J. Wang, S. Sun, X. Li, G. Fei, Z. Wang, H. Xia, *Manufacturing* **2023**, *10*, 684.
[209] A. Chortos, E. Hajiesmaili, J. Morales, D. R. Clarke, J. A. Lewis, *Adv. Funct. Mater.* **2020**, *30*, 1907375.
[210] M. Shahinpoor, K. J. Kim, *Smart Mater. Struct.* **2001**, *10*, 819.
[211] J. D. Carrico, N. W. Traeden, M. Aureli, K. K. Leang, *Smart Mater. Struct.* **2015**, *24*, 125021.
[212] N. Kellaris, V. Gopaluni Venkata, G. M. Smith, S. K. Mitchell, C. Keplinger, *Sci. Rob.* **2018**, *3*, eaar3276.
[213] P. Rothemund, N. Kellaris, S. K. Mitchell, E. Acome, C. Keplinger, *Adv. Mater.* **2021**, *33*, 2003375.
[214] R. Niiyama, D. Rus, S. Kim, in *2014 IEEE Int. Conf. Robotics and Automation (ICRA)*, IEEE, Hong Kong, China, September **2014**, pp. 6332–6337.
[215] M. R. O'Neill, E. Acome, S. Bakarich, S. K. Mitchell, J. Timko, C. Keplinger, R. F. Shepherd, *Adv. Funct. Mater.* **2020**, *30*, 2005244.
[216] Y. Zhang, N. Zhang, H. Hingorani, N. Ding, D. Wang, C. Yuan, B. Zhang, G. Gu, Q. Ge, *Adv. Funct. Mater.* **2019**, *29*, 1806698.
[217] K. Autumn, *MRS Bull.* **2007**, *32*, 473.
[218] S. Song, D. M. Drotlef, C. Majidi, M. Sitti, *Proc. Natl. Acad. Sci. U.S.A.* **2017**, *114*, E4344.
[219] A. Davoudinejad, M. M. Ribo, D. B. Pedersen, A. Islam, G. Tosello, *J. Micromech. Microeng.* **2018**, *28*, 085009.
[220] C. B. Dayan, S. Chun, N. Krishna-Subbaiah, D. Drotlef, M. B. Akolpoglu, M. Sitti, *Adv. Mater.* **2021**, *33*, 2103826.
[221] J. Shintake, V. Cacucciolo, D. Floreano, H. Shea, *Adv. Mater.* **2018**, *30*, 1707035.
[222] Y. Yang, K. Jin, H. Zhu, G. Song, H. Lu, L. Kang, *Micromachines* **2021**, *12*, 1141.
[223] Y. Jiang, Y. Li, K. Liu, H. Zhang, X. Tong, D. Chen, L. Wang, J. Paik, *Cell Rep. Phys. Sci.* **2023**, *4*, 101365.
[224] A. H. Chu, T. Cheng, A. Muralt, C. D. Onal, *Soft Rob.* **2023**, *10*, 556.
[225] K. C. Galloway, K. P. Becker, B. Phillips, J. Kirby, S. Licht, D. Tchernov, R. J. Wood, D. F. Gruber, *Soft Rob.* **2016**, *3*, 23.
[226] Y. Yang, K. Vella, D. P. Holmes, *Sci. Rob.* **2021**, *6*, eabd6426.
[227] G. Kang, Y. J. Kim, S. J. Lee, S. K. Kim, D. Y. Lee, K. Song, *Nat. Commun.* **2023**, *14*, 4633.
[228] Y. Hong, Y. Zhao, J. Berman, Y. Chi, Y. Li, H. Huang, J. Yin, *Nat. Commun.* **2023**, *14*, 4625.
[229] Y. Zhang, W. Zhang, P. Gao, X. Zhong, W. Pu, *Nat. Commun.* **2022**, *13*, 7700.
[230] C. Tawk, M. in het Panhuis, G. M. Spinks, G. Alici, *Soft Rob.* **2018**, *5*, 685.
[231] C. Yoon, *Nano Convergence* **2019**, *6*, 20.
[232] Z. Guan, L. Wang, J. Bae, *Mater. Horiz.* **2022**, *9*, 1825.
[233] L. Zhang, X. Huang, T. Cole, H. Lu, J. Hang, W. Li, S.-Y. Tang, C. Boyer, T. P. Davis, R. Qiao, *Nat. Commun.* **2023**, *14*, 7815.
[234] H. Son, E. Byun, Y. J. Yoon, J. Nam, S. H. Song, C. Yoon, *ACS Macro Lett.* **2020**, *9*, 1766.
[235] M. Tyagi, G. M. Spinks, E. W. Jager, *Soft Rob.* **2021**, *8*, 19.
[236] F. Zhou, M. Zhang, X. Cao, Z. Zhang, X. Chen, Y. Xiao, Y. Liang, T.-W. Wong, T. Li, Z. Xu, *Sens. Actuators, A* **2019**, *292*, 112.
[237] A. Koivikko, D.-M. Drotlef, C. B. Dayan, V. Sariola, M. Sitti, *Adv. Intell. Syst.* **2021**, *3*, 2100034.
[238] C. Xiang, Y. Guan, H. Zhu, S. Lin, Y. Song, *Sens. Actuators, A* **2022**, *344*, 113747.
[239] J. Zhang, J. Sheng, C. T. O'Neill, C. J. Walsh, R. J. Wood, J.-H. Ryu, J. P. Desai, M. C. Yip, *IEEE Trans. Rob.* **2019**, *35*, 761.
[240] H. Liu, C. Wu, S. Lin, Y. Chen, Y. Hu, T. Xu, W. Yuan, Y. Li, *Adv. Intell. Syst.* **2023**, *5*, 2200274.
[241] D. Sangian, A. Jeiranikhameneh, S. Naficy, S. Beirne, G. M. Spinks, *3D Print. Addit. Manuf.* **2019**, *6*, 57.
[242] T. J. Jones, E. Jambon-Puillet, J. Marthelot, P. T. Brun, *Nature* **2021**, *599*, 229.
[243] W. Hu, G. Alici, *Soft Rob.* **2020**, *7*, 267.
[244] H. Ur Rehman, Y. Chen, M. S. Hedenqvist, H. Li, W. Xue, Y. Guo, Y. Guo, H. Duan, H. Liu, *Adv. Funct. Mater.* **2017**, *28*, 1704109.
[245] E. Farber, J. N. Zhu, A. Popovich, V. Popovich, *Mater. Today: Proc.* **2020**, *30*, 761.
[246] M. Sui, Y. Ouyang, H. Jin, Z. Chai, C. Wei, J. Li, M. Xu, W. Li, L. Wang, S. Zhang, *Nat. Mach. Intell.* **2023**, *5*, 1149.
[247] Y. Wang, X. Ma, Y. Jiang, W. Zang, P. Cao, M. Tian, N. Ning, L. Zhang, *Resour. Chem. Mater.* **2022**, *1*, 308.
[248] A. Chortos, J. Mao, J. Mueller, E. Hajiesmaili, J. A. Lewis, D. R. Clarke, *Adv. Funct. Mater.* **2021**, *31*, 2010643.
[249] C. A. Manion, D. K. Patel, M. Fuge, S. Bergbrieter, in *Int. Conf. on Intelligent Robots and Systems (IROS)*, IEEE, Madrid, Spain, October **2018**.
[250] I. H. Kim, S. Choi, J. Lee, J. Jung, J. Yeo, J. T. Kim, S. Ryu, S. Ahn, J. Kang, P. Poulin, S. O. Kim, *Nat. Nanotechnol.* **2022**, *17*, 1198.
[251] T. J. Buchner, S. Rogler, S. Weirich, Y. Armati, B. G. Cangan, J. Ramos, S. T. Twiddy, D. M. Marini, A. Weber, D. Chen, G. Ellson, J. Jacob, W. Zengerle, D. Katalichenko, C. Keny, W. Matusik, R. K. Katzschmann, *Nature* **2023**, *623*, 522.

[252] X. Sheng, H. Xu, N. Zhang, N. Ding, X. Zhu, G. Gu, *Sens. Actuators, A* **2020**, *316*, 112398.
[253] Y. Yang, H. Zhu, J. Liu, H. Lu, Y. Ren, M. Y. Wang, *Polymers* **2022**, *14*, 2265.
[254] T. Umedachi, V. Vikas, B. A. Trimmer, *Bioinspiration Biomimetics* **2016**, *11*, 025001.
[255] G. Gu, J. Zou, R. Zhao, X. Zhao, X. Zhu, *Sci. Rob.* **2018**, *3*, eaat2874.
[256] H.-C. Fu, J. D. L. Ho, K.-H. Lee, Y. C. Hu, S. K. W. Au, K.-J. Cho, K. Y. Sze, K.-W. Kwok, *Soft Rob.* **2020**, *7*, 44.
[257] H. T. Lin, G. G. Leisk, B. Trimmer, *Bioinspiration Biomimetics* **2011**, *6*, 026007.
[258] S. Fu, L. Shen, J. Qu, J. Xia, W. Xie, Y. Li, H. Liu, T. Ren, Y. Yang, *IEEE Rob. Autom. Lett.* **2024**, *9*, 8897.
[259] W.-B. Li, W.-M. Zhang, H.-X. Zou, Z.-K. Peng, G. Meng, *IEEE/ASME Trans. Mechatron.* **2018**, *23*, 1630.
[260] J. Wang, Y. Fei, Z. Liu, *Mechatronics* **2019**, *57*, 150.
[261] C. Y. Yeh, C. Y. Chen, J. Y. Juang, *Extreme Mech. Lett.* **2020**, *39*, 100854.
[262] Y. Lin, Y. X. Xu, J. Y. Juang, *Soft Rob.* **2023**, *10*, 174.
[263] D. Xie, J. Liu, R. Kang, S. Zuo, *IEEE Rob. Autom. Lett.* **2021**, *6*, 462.
[264] P. Singh Matharu, Z. Wang, J. H. Costello, S. P. Colin, R. H. Baughman, Y. T. Tadesse, *Ocean Eng.* **2023**, *279*, 114427.
[265] P. Phamduy, M. A. Vazquez, C. Kim, V. Mwaffo, A. Rizzo, M. Porfiri, *Int. J. Intell. Rob. Appl.* **2017**, *1*, 209.
[266] K. Y. Lee, L. Wang, J. Qu, K. R. Oldham, in *Int. Conf. on Manipulation, Automation and Robotics at Small Scales (MARSS)*, IEEE, Helsinki, Finland, July **2019**, pp. 1–6.
[267] L. Sun, J. Wan, T. Du, *Bioinspiration Biomimetics* **2023**, *18*, 066011.
[268] Y. Yang, Y. Xie, J. Liu, Y. Li, F. Chen, *Soft Rob.* **2024**, *11*, 650.
[269] C. Richter, H. Lipson, *Artif. Life* **2011**, *17*, 73.
[270] N. Meiri, D. Zarrouk, in *2019 Int. Conf. Robotics and Automation (ICRA)*, IEEE, Montreal, Canada, May **2019**, pp. 5302–5308.
[271] B. B. Kang, H. Choi, H. Lee, K. J. Cho, *Soft Rob.* **2019**, *6*, 214.
[272] J. Xia, Y. Li, S. Fu, W. Xie, J. Qu, Y. Li, T. Ren, Y. Yang, H. Liu, *Smart Mater. Struct.* **2024**, *33*, 045018.
[273] S. Walker, A. Firouzeh, M. Robertson, Y. Mengüç, J. Paik, *Soft Rob.* **2022**, *9*, 354.
[274] S. J. Lee, H. H. Jo, K. S. Lim, D. Lim, S. Lee, J. H. Lee, W. D. Kim, M. H. Jeong, J. Y. Lim, I. K. Kwon, Y. Jung, J.-K. Park, S. A. Park, *Chem. Eng. J.* **2019**, *378*, 122116.
[275] Z. Chen, Z. Jin, L. Yang, Y. Liu, J. Liu, S. Cai, Y. Shen, S. Guo, *Mater. Today Chem.* **2022**, *24*, 100760.
[276] A. Mohammadi, J. Lavranos, H. Zhou, R. Mutlu, G. Alici, Y. Tan, P. Choong, D. Oetomo, *PLoS One* **2020**, *15*, 0232766.
[277] K. Wang, C. C. Ho, C. Zhang, B. Wang, *Engineering* **2017**, *3*, 653.
[278] J. Wang, Y. Zhang, N. H. Aghda, A. R. Pillai, R. Thakkar, A. Nokhodchi, M. Maniruzzaman, *Adv. Drug Delivery Rev.* **2021**, *174*, 294.
[279] X. Yang, W. Shang, H. Lu, Y. Liu, L. Yang, R. Tan, X. Wu, Y. Shen, *Sci. Rob.* **2020**, *5*, eabc8191.
[280] H. Li, G. Go, S. Y. Ko, J.-O. Park, S. Park, *Smart Mater. Struct.* **2016**, *25*, 027001.
[281] P. Cabanach, A. Pena-Francesch, D. Sheehan, U. Bozuyuk, O. Yasa, S. Borros, M. Sitti, *Adv. Mater.* **2020**, *32*, 2003013.
[282] S. R. Khan, M. P. Desmulliez, *Micromachines* **2019**, *10*, 545.
[283] M. Cianchetti, C. Laschi, A. Menciassi, P. Dario, *Nat. Rev. Mater.* **2018**, *3*, 143.
[284] Y. Hu, L. Zhang, W. Li, G. Z. Yang, *IEEE Rob. Autom. Lett.* **2019**, *4*, 1557.
[285] G. Fang, M. C. Chow, J. D. Ho, Z. He, K. Wang, T. C. Ng, J. K. Tsoi, P.-L. Chan, H.-C. Chang, D. T.-M. Chan, Y. Liu, F. C. Holsinger, J. Y.-K. Chan, K.-W. Kwok, *Sci. Rob.* **2021**, *6*, eabg5575.
[286] D. B. Comber, J. E. Slightam, V. R. Gervasi, J. S. Neimat, E. J. Barth, *IEEE Trans. Rob.* **2016**, *32*, 138.
[287] G. L. Goh, W. Y. Yeong, J. Altherr, J. Tan, D. Campolo, *Mater. Today: Proc.* **2022**, *70*, 224.
[288] Y. Xin, X. Zhou, H. Bark, P. S. Lee, *Adv. Mater.* **2023**, *36*, 2307963.
[289] Y. Wu, Z. Wang, G. Zeng, Z. Xu, Z. Hai, Z. Chen, Y. Zhao, D. Wu, *Adv. Eng. Mater.* **2022**, *24*, 2200704.
[290] M. Kang, J. Kim, B. Jang, Y. Chae, J.-H. Kim, J.-H. Ahn, *ACS Nano* **2017**, *11*, 7950.
[291] M. A. Ragolia, A. M. Lanzolla, G. Percoco, G. Stano, A. Di Nisio, *Sensors* **2021**, *21*, 6324.
[292] X. Zhou, K. Parida, O. Halevi, Y. Liu, J. Xiong, S. Magdassi, P. S. Lee, *Nano Energy* **2020**, *72*, 104676.
[293] M. A. Mahmud, A. Zolfagharian, S. Gharaie, A. Kaynak, S. H. Farjana, A. V. Ellis, J. Chen, A. Z. Kouzani, *Adv. Energy Sustainability Res.* **2021**, *2*, 2000045.
[294] M. Zhu, M. Xie, X. Lu, S. Okada, S. Kawamura, *Nano Energy* **2020**, *73*, 104772.
[295] J. Wan, H. Wang, L. Miao, X. Chen, Y. Song, H. Guo, C. Xu, Z. Ren, H. Zhang, *Nano Energy* **2020**, *74*, 104878.
[296] H. Zhao, K. O'brien, S. Li, R. F. Shepherd, *Sci. Rob.* **2016**, *1*, eaai7529.
[297] T. An, S. Yoon, J. Kim, *Addit. Manuf.* **2023**, *71*, 103600.
[298] M. Sitti, *Extreme Mech. Lett.* **2021**, *46*, 101340.
[299] Y. Zhang, Z. Qian, J. Zhuang, S. Fan, H. Wei, N. Yang, *Adv. Intell. Syst.* **2023**, *5*, 2200374.
[300] D. J. Preston, P. Rothemund, H. J. Jiang, M. P. Nemitz, J. Rawson, Z. Suo, G. M. Whitesides *Proc. Natl. Acad. Sci. U.S.A.* **2019**, *116*, 7750.
[301] P. Rothemund, A. Ainla, L. Belding, D. J. Preston, S. Kurihara, Z. Suo, G. M. Whitesides, *Sci. Rob.* **2018**, *3*, eaar7986.
[302] S. Conrad, J. Teichmann, P. Auth, N. Knorr, K. Ulrich, D. Bellin, T. Speck, F. J. Tauber, *Sci. Rob.* **2024**, *9*, eadh4060.
[303] J. D. Hubbard, R. Acevedo, K. M. Edwards, A. T. Alsharhan, Z. Wen, J. Landry, K. Wang, S. Schaffer, R. D. Sochol, *Sci. Adv.* **2021**, *7*, eabe5257.
[304] S. Wang, L. He, Y. Yao, C. Liu, P. Maiolino, *Adv. Intell. Syst.* **2023**, *5*, 2300394.
[305] Q. He, R. Yin, Y. Hua, H. Shu, X. Zhu, A. T. Haque, S. Ferracin, S. Patel, W. Jiao, J. R. Raney, *Adv. Intell. Syst.* **2024**, 2400659. 10.1002/aisy.202400659.
[306] E. W. Hawkes, L. H. Blumenschein, J. D. Greer, A. M. Okamura, *Sci. Rob.* **2017**, *2*, eaan3028.
[307] A. Sadeghi, A. Mondini, B. Mazzolai, *Soft Rob.* **2017**, *4*, 211.
[308] A. Sadeghi, E. Del Dottore, A. Mondini, B. Mazzolai, *Soft Rob.* **2020**, *7*, 85.
[309] E. Del Dottore, A. Mondini, N. Rowe, B. Mazzolai, *Sci. Rob.* **2024**, *9*, eadi5908.
[310] M. M. Hausladen, B. Zhao, M. S. Kubala, L. F. Francis, T. M. Kowalewski, C. J. Ellison, *Proc. Natl. Acad. Sci. U.S.A.* **2022**, *119*, e2201776119.
[311] W. Zhu, C. Lu, Q. Zheng, Z. Fang, H. Che, K. Tang, M. Zhu, S. Liu, Z. Wang, *IEEE/ASME Trans. Mechatron.* **2022**, *28*, 104.
[312] Z. Xie, F. Yuan, J. Liu, L. Tian, B. Chen, Z. Fu, S. Mao, T. Jin, Y. Wang, X. He, G. Wang, Y. Mo, X. Ding, Y. Zhang, C. Laschi, L. Wen, *Sci. Rob.* **2023**, *8*, eadh7852.
[313] C. Tawk, R. Mutlu, G. Alici, *Front. Rob. AI* **2022**, *8*, 799230.
[314] W. Hu, G. Z. Lum, M. Mastrangeli, M. Sitti, *Nature* **2018**, *554*, 81.
[315] R. Baines, S. K. Patiballa, J. Booth, L. Ramirez, T. Sipple, A. Garcia, F. Fish, R. Kramer-Bottiglio, *Nature* **2022**, *610*, 283.
[316] M. Zhang, X. Fan, L. Dong, C. Jiang, O. Weeger, K. Zhou, D. Wang, *Adv. Sci.* **2024**, *11*, 2309932.

[317] Z. Bai, L. Zhang, X. Zhou, S. Zhao, C. Yang, Y. Zhou, K. Tan, Z. Zhao, H. Chen, *Adv. Mater. Technol.* **2023**, *9*, 2301150.
[318] A. R. Sani, A. Zolfagharian, A. Z. Kouzani, *Adv. Intell. Syst.* **2024**, *6*, 2400102.
[319] Z. Zhu, D. W. H. Ng, H. S. Park, M. C. McAlpine, *Nat. Rev. Mater.* **2021**, *6*, 27.
[320] E. Kanhere, T. Calais, S. Jain, A. R. Plamootil Mathai, A. Chooi, T. Stalin, V. S. Joseph, P. Valdivia y Alvarado, *Sci. Rob.* **2024**, *9*, eadn4542.
[321] Z. Wang, N. M. Freris, X. Wei, *Device* **2024**, 0, 100646. 10.1016/j.device.2024.100646.
[322] G. Hiramandala, T. Calais, T. Stalin, A. Chooi, A. P. Mathai, S. Jain, E. V. Kanhere, P. Valdivia y Alvarado, in *2023 IEEE Int. Conf. on Soft Robotics (RoboSoft)*, IEEE, Singapore, April **2023**, pp. 1–7.
[323] J. Plog, X. Wang, Y. Pan, A. L. Yarin, *J. Manuf. Processes* **2022**, *76*, 752.
[324] D. K. Limberg, J. H. Kang, R. C. Hayward, *J. Am. Chem. Soc.* **2022**, *144*, 5226.
[325] B. Derby, *Annu. Rev. Mater. Res.* **2010**, *40*, 395.
[326] H. K. Yap, H. Y. Ng, C. H. Yeow, *Soft Rob.* **2016**, *3*, 144.
[327] J. Cheng, R. Wang, Z. Sun, Q. Liu, X. He, H. Li, H. Ye, X. Yang, X. Wei, Z. Li, B. Jian, W. Deng, Q. Ge, *Nat. Commun.* **2022**, *13*, 7931.
[328] J. Xia, J. Huang, S. Fu, J. Qu, L. Mo, Y. Li, T. Ren, Y. Yang, H. Liu, *Adv. Intell. Syst.* **2024**, 2400533. 10.1002/aisy.202400533.
[329] Z. Yoder, D. Macari, G. Kleinwaks, I. Schmidt, E. Acome, C. Keplinger, *Adv. Funct. Mater.* **2023**, *33*, 2209080.
[330] L. Mo, W. Xie, J. Qu, J. Xia, Y. Li, Y. Zhang, T. Ren, Y. Yang, J. Yi, C. Wu, Y. Chen, *Adv. Intell. Syst.* **2024**, *7*, 2400285.
[331] C. Linghu, S. Zhang, C. Wang, K. Yu, C. Li, Y. Zeng, H. Zhu, X. Jin, Z. You, J. Song, *Sci. Adv.* **2020**, *6*, eaay5120.
[332] M. Behl, K. Kratz, J. Zotzmann, U. Nöchel, A. Lendlein, *Adv. Mater.* **2013**, *32*, 4466.
[333] J. Shintake, S. Rosset, B. Schubert, D. Floreano, H. Shea, *Adv. Mater.* **2016**, *28*, 231.
[334] W. Ruotolo, D. Brouwer, M. R. Cutkosky, *Sci. Rob.* **2021**, *6*, eabi9773.

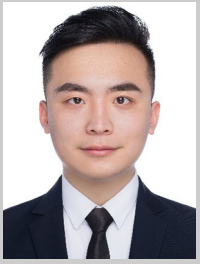

Hao Liu completed his undergraduate studies at the China University of Petroleum (East China) (B.Sc) and M.Sc. at the University of Hong Kong respectively. He is currently working toward his Ph.D. in mechanical engineering at the University of Hong Kong. His research interests include soft robotics, wearable robotics, and additive manufacturing.

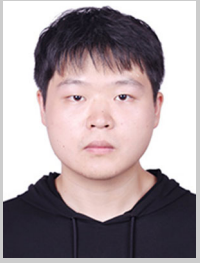

Changchun Wu completed his undergraduate studies at Chongqing University (B.Sc.), China, and the University of Cincinnati (B.Sc.), USA. He got his M.Sc. from the University of Hong Kong. He is currently working toward Ph.D. in mechanical engineering at the University of Hong Kong. His research interests include braided soft robotics and shape-morphing materials.

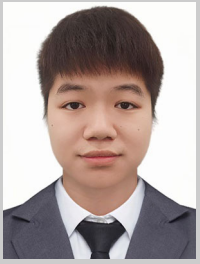

Senyuan Lin completed his undergraduate studies at South China Agricultural University (B.Sc) and M.Sc. from the University of Hong Kong. He is currently working toward Ph.D. in mechanical engineering at the University of Hong Kong. His research interests include humanoid robotics and service robotics.

James Lam received his B.Sc. in mechanical engineering from the University of Manchester in 1983 and his M.Phil. and Ph.D. from the University of Cambridge in 1985 and 1988, respectively. Before joining The University of Hong Kong, he was a lecturer with the City University of Hong Kong and the University of Melbourne. He is currently a Chair Professor of Control Engineering at the University of Hong Kong. His research interests include model reduction, robust synthesis, delay, singular systems, stochastic systems, multidimensional systems, positive systems, networked control systems, and vibration control.

Ning Xi received his D.Sc. from Washington University in 1993. He is the Chair Professor of Robotics and Automation in the Department of Data and Systems Engineering and the Director of the Advanced Technologies Institute, The University of Hong Kong. Before joining The University of Hong Kong, he was a university distinguished professor and the John D. Ryder Professor at Michigan State University. He served as the founding head of the Department of Mechanical and Biomedical Engineering, City University of Hong Kong. His research interests include robotics, manufacturing automation, micro/nanomanufacturing, nanosensors and devices, and intelligent control and systems.

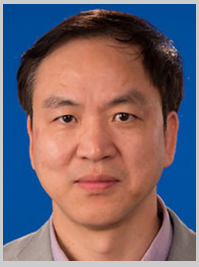

Yonghua Chen received his B.Sc. in mechanical engineering from Southwest Jiaotong University in 1985 and Ph.D. in mechanical engineering from the University of Liverpool in 1990. He is currently an associate professor at the Department of Mechanical Engineering, The University of Hong Kong, Hong Kong. Before joining The University of Hong Kong, he was with Motorola Electronics Pte, Ltd., Singapore; Asia Matsushita Electronics Pte, Ltd., Singapore; and Swire Technologies Pte, Ltd., Hong Kong, where he acquired experience in automation and robotics. His research interests include service robotics, soft robotics, and additive manufacturing.